Design and Development of an Advanced Coherent Radar Depth Sounder

Saikiran P. V. Namburi

B.Tech (Electronics and Communication Engineering), J.N.T.U,

Hyderabad, India - 2000

Submitted to the Department of Electrical Engineering and Computer Science and the Faculty of the Graduate School of the University of Kansas in partial fulfillment of the requirements for the degree of Master of Science.

_____
Committee Chairman

_____
Committee Member

_____
Committee Member

July 16, 2003
Date Thesis Presented

ACKNOWLEDGEMENTS

I would like to thank Dr. Prasad Gogineni for giving me the opportunity to work on this research project. I would like to thank him for his guidance and support throughout my career as a Research Assistant. I would like to thank Dr. Chris Allen and Dr. Glenn Prescott for serving on my thesis committee. I would like to acknowledge the support provided by NASA through Grant #NAG5-12439 ("Radar Soundings and Airborne High-Resolution Mapping of Near-Surface Layers of the Greenland Ice Sheet").

I take this opportunity to thank Dr. Pannirselvam Kanagaratnam and Torry Akins for helping me during the radar testing. I would like to thank Dennis Sundermeyer and Dan Depardo for helping me with the radar assembly. I would like to thank Kelly Mason for editing this thesis and for her help throughout my thesis.

I would like to thank all the students in the Greenland group for their help and support throughout my thesis. I thank all my friends at KU for making my stay in Lawrence a plesant and memorable one. Finally, I would like to thank my parents for their encouragement in completing this work.

ABSTRACT

In 1993 NASA initiated a program to assess the mass balance of the Greenland ice sheet. Since then the University of Kansas has used the coherent radar depth sounder for measuring the ice thickness. The depth sounder has been unsuccessful in measuring ice thickness over transition zones and a few outlet glaciers located in southern Greenland, where the off-vertical surface clutter or the multiple-time-around surface echoes mask the weak basal returns.

The existing depth sounder uses complementary Surface Acoustic Wave (SAW) devices to generate the transmitted chirp and compress the received signal. The peak range sidelobe in the compressed waveform is 26 dB below the main lobe. The current receiver employs a mechanism called Sensitivity Time Control (STC) to provide high dynamic range. Any imbalance between the in-phase (I) and quadrature-phase (Q) signals of the receiver will degrade the dynamic range. It was decided to develop a new system that eliminates the above problems.

The new system, Advanced COherent Radar Depth Sounder (ACORDS), was completely redesigned and rebuilt. A Waveform Generator (WG) was designed and developed to reduce the range sidelobes. A transmitter sub-system was developed to amplify the chirp signal up to 2 W peak power. A dual-channel receiver with two different gain channels was designed to eliminate the time-varying gain and provide high dynamic range. The transmitter sub-system and the dual channel receiver were packaged in an 18'' x 24'' x 7'' chassis. This new system offers the flexibility to

control radar parameters such as pulse width, receiver gain and blanking signals digitally.

The performance of the ACORDS was tested in the laboratory. The results showed that the first range sidelobes are around 36 dB below the main lobe when the transmitted waveform is Hamming weighted and compressed with a baseband Hamming waveform. The new radar system was tested in Greenland during the 2003 field experiment.

TABLE OF CONTENTS

LIST OF FIGURES

LIST OF TABLES

CHAPTER 1

Introduction

1.1 Significance of ice measurements

Sea level rise is an important indicator of global climate change. Sea level has been increasing at about 2mm/year over the past century and may continue to do so. It is predicted to rise between 50 and 70 cm over this century. The effect of continued sea level rise can be devastating. Many coastal regions would be flooded, causing migration of people from those areas.

About half of the rise is reported to be caused by the thermal expansion of the ocean and melting of mountain glaciers [1]. The polar (Antarctic and Greenland) ice sheets are believed to be contributing the remainder of the sea level rise. These polar ice sheets account for 80% of the earth's fresh water and have a major role to play in the sea level rise. A key to quantifying their contribution is an accurate determination of the mass balance of these ice sheets. Ice thickness is an important parameter required to estimate the mass balance of the ice sheet and to study ice dynamics.

In 1993 NASA initiated a Program for Arctic Regional Climate Assessment (PARCA) to collect ice thickness data on the Greenland ice sheet. Since then the Radar Systems and Remote Sensing Laboratory (RSL) at the University of Kansas has been involved in the research program. The main purpose of the PARCA is to assess the mass balance of the Greenland ice sheet.

1.2 KU radar history

In the 1980s, KU developed a Coherent Antarctic Radar Depth Sounder (CARDS) intended for ice-sheet sounding in Antarctica [2]. The data processing system [3] consisted of two 8-bit A/D converters and a signal processing system capable of doing pre-coherent integrations.

In 1996, the Improved Coherent Antarctic Radar Depth Sounder (ICARDS) was developed. Though this system was able to eliminate the problems faced by CARDS, it used many connectorized parts and was big and bulky. This led to the development of the Next-Generation Coherent Radar Depth Sounder system (NG-CORDS), which is compact and small. A brief description of the ICARDS and NG-CORDS is given in Chuah [4]. This system uses RFICs and MMICs instead of connectorized components. It also includes an improved data acquisition system [5] using 12-bit A/D converters. The NG-CORDS along with the new data acquisition system has been used in all the field experiments since 1998.

With these radars, we obtained good quality ice thickness data over 90% of the flight lines flown [6]. The processed data, the radar echograms and the derived ice thickness, were placed on a server at the University of Kansas (http://tornado.rsl.ku.edu/Greenlanddata.htm). We were unsuccessful in obtaining ice thickness data over a few outlet glaciers located in southern Greenland. The outlet glaciers play a major role in ice discharge and hence influence the mass balance of the ice sheets. Lack of good ice thickness data from the outlet glaciers has been an

impediment to accurately estimating ice discharge [7]. A new system needs to be built to address the above problems.

1.3 Organization

This thesis is organized into five chapters. Chapter 2 deals with the problems of the NG-CORDS and solutions to overcome them. The design and development of the radar and the digital system are described in Chapter 3. Chapter 4 evaluates the results of the new system during the 2003 field experiment. The concluding chapter contains some future recommendations to improve the performance of the radar.

CHAPTER 2

Background

The following sections will briefly describe the concept behind a chirp radar, the operation of the NG-CORDS, its limitations and solutions to overcome them.

2.1 Basic chirp radar

In a chirp radar, transmitter signal frequency increases or decreases linearly over the time duration (*T*) of each pulse. The received echo has the same linear increase or decrease in frequency. The received waveform is passed through the pulse-compression filter. The filter introduces a time lag that decreases linearly with frequency at the same rate as the linear increase in frequency or vice versa. Figure 2.1 shows the response of a pulse-compression filter to a chirped input pulse.

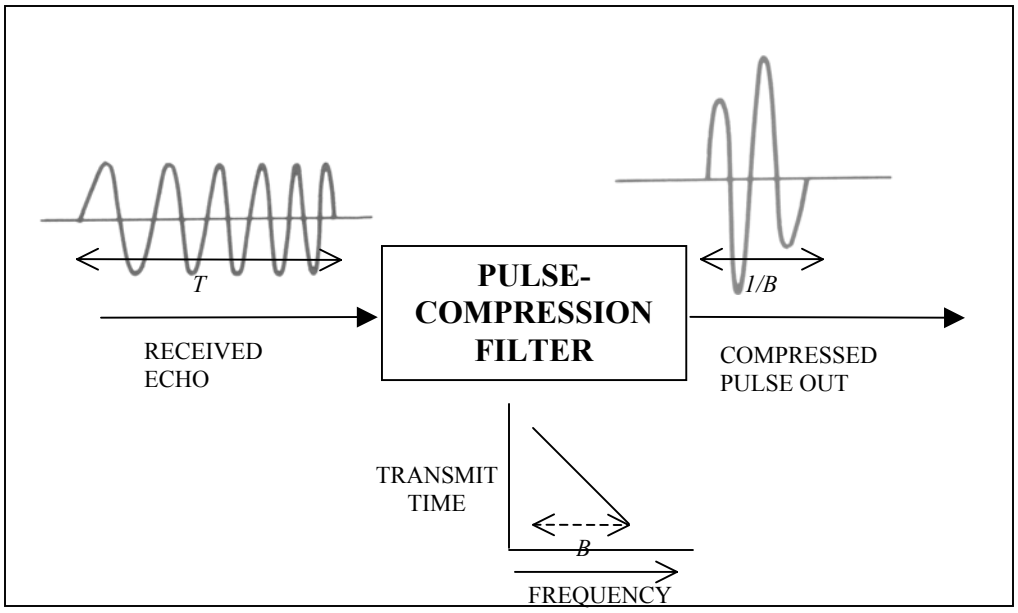

Figure 2.1: Response of a pulse-compression filter to a chirped input pulse

The need for pulse compression can be explained as follows. For any pulse radar, the energy contained in a single pulse and the range resolution are related to the pulse width, as shown in the following equation:

$$E = P \times T$$
$$r = \frac{C \times T}{2}, \tag{2.1}$$

where E is the energy per pulse, r is the range resolution of the radar, P is the peak transmit power, T is the pulse width of the chirp and C is the velocity of propagation in the medium.

It can be seen from the above equation that long pulse widths achieve high energy but have poor range resolution. On the other hand, shorter pulse widths will have good range resolution but less peak energy. In order to achieve high energy and good range resolution, radars employ pulse compression techniques. In pulse compression radar, a frequency modulated (FM) long pulse is transmitted to achieve high energy. On reception, a matched filter in the receiver compresses the long pulse to a width equal to *1/B*. The pulse compression ratio is defined as the ratio of the long pulse width T to the compressed pulse width τ. A more detailed explanation of chirped pulse compression can be found in Stimson [8].

2.2 NG-CORDS

Chuah [4] provided a detailed description of the NG-CORDS. It is an airborne radar that uses complementary Surface-Acoustic-Wave (SAW) devices [9] for both signal generation and matched filtering of a linear chirp waveform.

The NG-CORDS transmitter generates a linear frequency modulated chirp from 140-160 MHz over the duration of 1.6 μs with a peak transmit power of 200 W. The radar uses two identical four-element dipole antenna arrays as transmit and receiver antennas. The radar system along with the host computer is mounted in an instrument rack inside the aircraft and connected to the antennas. The NG-CORDS receiver, with an overall gain of about 90 dB, filters, amplifies and compresses the received signals before they are digitized. The NG-CORDS digital system consists of two 12-bit A/D converters and digitizes the in-phase (I) and quadrature (Q) output signals from the receiver. Table 2.1 shows the system parameters of the NG-CORDS.

Description	**Characteristic**	**Units**
Radar Type	Pulse Compression	----
RF Carrier Frequency	150	MHz
RF Up-Chirp Bandwidth	17.00	MHz
Transmitted Pulse Width	1.6	μs
Compressed Pulse Width	60	ns
Range Sidelobes	< 26	dB
Peak Transmit Power	200	W
PRF	Selectable	KHz
Number of Coherent Integrations	32 – 4,096	----
Number of Incoherent Integrations	0 – 64,000	----
A/D Dynamic Range	12-bit, 72	dB
Sampling Period	53.3 (18.75 MHz)	ns
Range Resolution	4.494	m
Antennas	4-element λ/2 dipole arrays	

Table 2.1: System parameters of the NG-CORDS

2.2.1 Limitations of the NG-CORDS

The NG-CORDS has been used for measuring ice thickness in KU's field experiments from 1998 to 2002. During these experiments we were successful in obtaining the ice thickness for 90% of the flight lines flown [6]. We were unsuccessful in obtaining the ice thickness over a few outlet glaciers in southern Greenland and over transition zones. In the case of the outlet glaciers, off-vertical surface clutter masked the weak returns from the ice/bedrock interface. A transition zone is an area where the ice slowly transitions into the ocean. In these areas where the ice thickness is shallow, the multiple-time-around surface echoes mask the basal returns. The following section deals with limitations of the NG-CORDS.

2.2.1.1 Range sidelobes

Range sidelobes are produced at the output of the pulse compression filter in the receiver. The output of the pulse compression filter is the autocorrelation of the input chirp, thus resulting in time sidelobes or range sidelobes [10]. The time extent of the range sidelobes is approximately equal to the chirp pulse width. The envelope output of the matched filter for an ideal input chirp has peak range sidelobes that are 13.2 dBc below the main lobe.

In the NG-CORDS receiver, the Band Pass Filters (BPF) located before the SAW compressor shape the received pulse. Thus the peak range sidelobes in the NG-CORDS receiver are 26 dBc below the main lobe. These range sidelobes can be mistaken for targets and can mask the weak returns from the bedrock. The smaller the range sidelobes, the better the performance of the radar system.

Weighting the uncompressed pulse can reduce the range sidelobes. Weighting will widen the compressed pulse, hence degrading the range resolution of the radar. But this is a small price to pay for the reduction in the range sidelobes. Thus there is a tradeoff between the radar range resolution and the range sidelobes.

2.2.1.2 Sensitivity Time Control

Chuah [4] has shown that the two-way ice attenuation in the Greenland ice sheet can be as much as 80 dB. Sensitivity Time Control (STC) is a mechanism used in the NG-CORDS receiver to increase the dynamic range of the receiver. The dynamic range of the STC is at least 32 dB and it attenuates the strong returns from the air/ice interface by 32 dB.

The effect of the STC gain sometimes leads to loss of the layering information in the radar echograms. The STC curve is panel-adjustable and is set by the radar operator. As this waveform is not stored, it becomes difficult later on to determine the actual gain setting of the receiver.

2.2.1.3 Analog down conversion

Another limitation in the NG-CORDS receiver is the effect of I-Q down-converters on the dynamic range of the receiver. If the I-Q signals are not perfectly balanced in phase and amplitude, an image signal is created that can significantly limit the dynamic range of the receiver. Reduction in the dynamic range of the receiver will degrade the sensitivity of the radar system.

2.2.2 Solutions for the NG-CORDS

2.2.2.1 Mismatched filter approach

The solution to the range sidelobes is to design a system in which the range sidelobes are further reduced. They can be reduced by amplitude weighting of the transmitted chirp. A detailed description of the various windowing functions that can be used is given in Harris [11]. A mismatched filter approach [12] can be used to reduce the sidelobe level significantly. In this approach the spectrum of the transmitted waveform, *X(f)*, is given as

$$X(f) = \frac{Y(f)}{H(f)} \quad , \tag{2.2}$$

where *Y(f)* is the output spectrum that is assumed to be a particular window and *H(f)* is the transfer function of the transceiver.

Thus a transmitter that can generate the above waveform needs to be designed.

2.2.2.2 Dual channel receiver

The easiest way to get rid of the STC is to design a dual-channel receiver with two different gain channels, a Low Gain (LG) and a High Gain (HG) channel. The strong returns from the air/ice interface and a few internal layers will be recorded in the LG channel, whereas the weak returns will be recorded in the HG channel.

2.2.2.3 Digital down conversion

As the bandwidth of the transmitted chirp is only 20 MHz, the received echoes can be digitally down converted using bandpass sampling techniques. The aliasing

action in bandpass sampling can be used to translate the radio frequency (RF) signal down to the baseband. This will get rid of the IQ demodulator and the local oscillator in the NG-CORDS receiver.

2.3 Need for an advanced radar system

Based on the above solutions, a need exists to develop a new radar system with the following features:

- Waveform Generator (WG) to generate a 140- to 160-MHz chirp using the mismatched filter approach.
- Dual-channel receiver with two different gain channels.
- Data acquisition system with two 12-bit A/D converters with large bandwidth that can operate at higher sampling frequencies.
- Capacity to generate all the control signals digitally, which will help make the radar system operator-friendly.
- Inexpensive and small size.

CHAPTER 3

Advanced COherent Radar Depth Sounder

3.1 System description

The main objectives of this new system that we called the Advanced COherent Radar Depth Sounder (ACORDS) are: 1) to generate the transmit waveform digitally by eliminating the SAW expander in the transmitter; 2) to design a dual-channel receiver with high dynamic range; 3) to control the whole system digitally.

An overview of ACORDS will be given in the following section. The derivation of improved specifications will be given in Section 3.2. The design process involved in the selection of clocks is given in Section 3.3. The transmitter and receiver designs are discussed in Sections 3.4 and 3.5 respectively. A brief description of the digital system is given in Section 3.6. The housing of the analog system is explained in Section 3.7. Section 3.8 deals with the experimental setup and also contains some results from the laboratory experiment.

3.1.1 System overview

The RSL ACORDS is an enhanced version of the NG-CORDS. It contains a digital and a radar system. The ACORDS is unique in the sense that it generates the transmit waveform digitally and uses bandpass sampling and digital pulse compression techniques. The system parameters of the ACORDS are tabulated in Table 3.1.

The block diagram of the ACORDS is shown in Figure 3.1. The radar system, consisting of a transmitter, power amplifier, dual-channel receiver, synchronization circuit and antennas, is shaded in light gray. The digital system, consisting of a rack mount host computer, waveform generator and data acquisition, is shaded in dark grey. The ACORDS digital system has been designed and developed by Torry Akins. The operation of the whole system is discussed below.

Description	**Characteristic**	**Units**
Radar Type	Pulse Compression	----
RF Carrier Frequency	150	MHz
RF Up-Chirp Bandwidth	17.00	MHz
Transmitted Pulse Width	Selectable (200nsec – 10usec)	μs
Range Sidelobes	< 36	dB
Peak Transmit Power	200	W
PRF	Selectable	KHz
Number of Coherent Integrations	32 – 1024	----
Number of Incoherent Integrations	0 – 64,000	----
A/D dynamic range	12-bit, 72	dB
Receiver Dynamic Range	>110	dB
Sampling Period	18.182 (55 MHz)	ns
Range Resolution	4.494	m
Antennas	4-element λ/2 dipole arrays	

Table 3.1: Radar system parameters of the ACORDS

The digital system of the ACORDS has been completely redesigned and rebuilt. The host computer controls the digital system through a Universal Serial Bus (USB) port. The digital system is used to: 1) generate a linear-chirp signal using a 110-MHz clock supplied by the transmitter; 2) generate all the blanking (control)

signals to control the switches in the radar system, referencing a 10-MHz clock signal supplied by the transmitter; 3) control the receiver gain by changing the attenuation in the two channels; 4) digitize and integrate the backscattered echoes (LG and HG returns from the receiver). The digitized data are then integrated before sending to the host computer where they are stored.

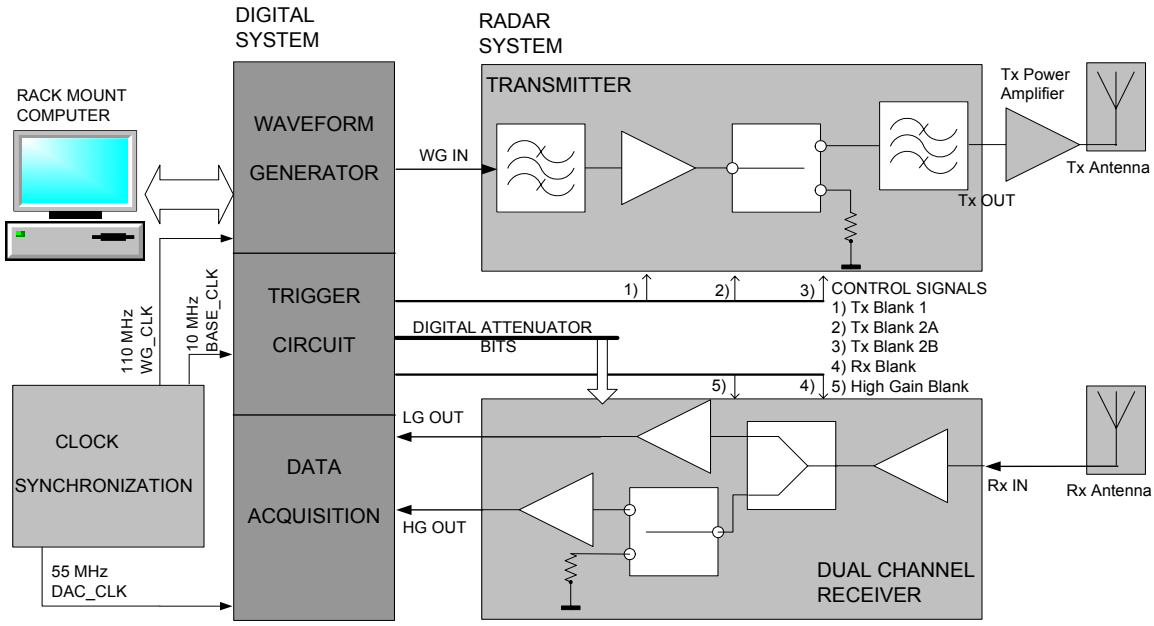

Figure 3.1: System block diagram of ACORDS

The synchronization circuit generates three clock signals: 1) a 10-MHz base clock for referencing the whole system; 2) a 110-MHz oversampling clock for the waveform generator; 3) a 55-MHz sampling clock for digitizing the received echoes.

The transmitter in the ACORDS is different from the NG-CORDS transmitter in that it does not generate the chirp pulse. In ACORDS, the chirp pulse is generated by the digital system, whereas it was generated in the transmitter in the NG-CORDS. The chirp pulse is amplified and filtered in the transmitter subsystem. The RF chirp pulse, however, is referenced to the PRF signal. To provide additional amplification,

an off-the-shelf 200-W amplifier is used as the power amplifier. The amplified RF chirp pulse is transmitted with a transmit antenna array consisting of four λ/2 dipoles.

The receiver has been completely redesigned and rebuilt. It amplifies the received signals and splits them into two parts: one of these is passed to the low-gain (LG) channel and the other into the high-gain (HG) channel. The receiver gain is selected digitally by controlling the attenuators in both the channels. The RF signals are digitized directly using a sampling technique called band-pass sampling.

3.1.2 Operation of the ACORDS

The operation of the ACORDS is shown in the timing diagram of Figure 3.2. The synchronization circuit in the radar system generates the base clock of 10 MHz. The waveform generator (WG) clock (110 MHz) and data acquisition (DAC) clock (55 MHz) are derived from the base clock using a phase-locked oscillator and a frequency divider. The trigger section in the digital system generates the pulse repetition frequency (PRF) and the entire set of control signals with reference to the base clock. Thus the waveform generator, radar system and the data acquisition are all synchronized to the 10-MHz crystal oscillator in the transmitter. The waveform generator synthesizes the RF chirp pulse each time it is triggered by the PRF. The blanking or control signals (Tx Blank 1, Tx Blank 2A, Tx Blank 2B) in the transmitter then modulate and shape the transmit chirp accordingly. These control signals are in the ON state for the duration of the transmit chirp pulse. The blanking signals (Rx Blank, High Gain Blank) in the receiver are set accordingly to protect the front end and high gain section of the receiver from saturation. The Rx Blank is in the

OFF state (Rx Blank at LOW state) during the transmission of the chirp pulse to prevent the leakage signal from damaging the receiver. The High Gain Blank is in the OFF state (signal at LOW state) to prevent the strong returns from the air/ice interface from saturating the amplifiers in the high-gain channel. The operator controls the duration for which the control signals are either ON or OFF digitally. The above process repeats itself after each pulse repetition period as long as the radar is on.

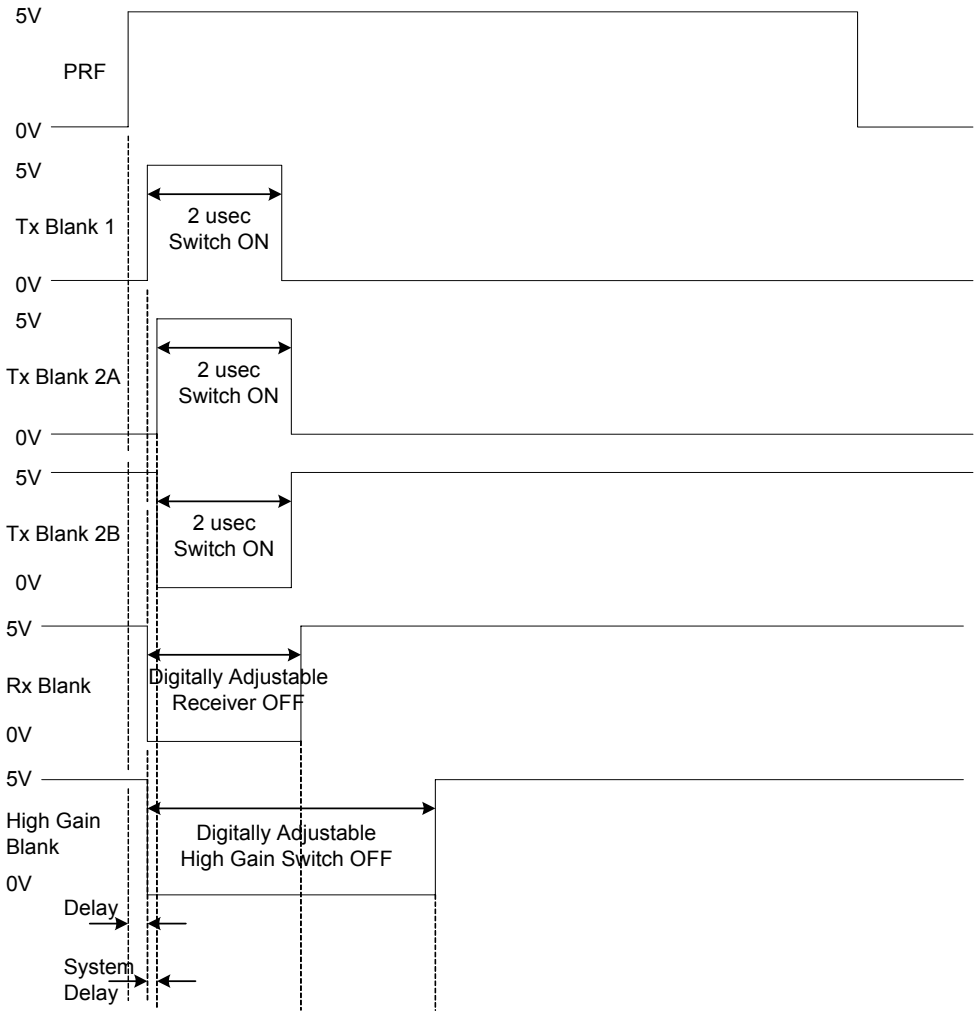

Figure 3.2: Timing diagram of the operation of ACORDS.

3.2 Derivation of improved specifications

3.2.1 Derivation of receiver gain

The ACORDS requires high loop sensitivity similar to that of the NG-CORDS to compensate for the spreading loss in free-space and the electromagnetic attenuation in ice. The receiver gain depends on parameters such as the A/D noise level, system noise and the signal processing gain. The following subsections deal with the derivation of the receiver gain in both the channels.

A/D noise level

The data acquisition system for the ACORDS uses a 12-bit A/D converter with a digitizing range of +0.5V to –0.5V. Based on the above specifications, the maximum signal level that can be digitized by the A/D in a 50Ω system is given by

$$P_{A/D\max} = \frac{V_{p-p}^2}{8*R} = \frac{1.0^2}{8*50} = 0.0025W = 4dBm \quad . \tag{3.1}$$

The quantization signal to noise ratio of the A/D converter is given by

$$SNR[dB] = 1.76 + 20 \times \log_{10} Q = 74dB \quad , \tag{3.2}$$

where Q, number of quantization levels = 2^n , and n, number of digitization bits = 12.

By taking into account the quantization losses, the effective SNR is assumed to be around 67 dB. We have the effective SNR of the A/D as 67 dB, and the maximum A/D signal level as 4 dBm. Thus the A/D noise level ($P_{A/Dnoise}$) is calculated as

$$P_{A/Dnoise}[dBm] = 4 - 67 = -63dBm \quad . \tag{3.3}$$

Receiver Noise

The product of the thermal noise and the receiver noise figure gives the receiver noise (system noise). It can be calculated as

$$N_{sys}[dBm] = N_{thermal} + NF_{recv} = kTB + F \quad , \tag{3.4}$$

where $N_{thermal}$ is the thermal noise (kTB), NF_{recv} is the receiver noise figure, k is the Boltzman constant ($1.38*10^{-23}$ Joule/degree), T is the equivalent noise temperature (290 K) and B is the system bandwidth (20 MHz).

The noise figure, NF_{recv}, of the receiver is given by

$$NF_{recv} = F_1 + \frac{F_2 - 1}{G_1} + \frac{F_3 - 1}{G_1 G_2} + \frac{F_4 - 1}{G_1 G_2 G_3} + \ldots + \frac{F_N - 1}{\prod_{n=1}^{N-1} G_n} \quad , \tag{3.5}$$

where F_n is the linear noise figure in the nth stage of the receiver and G_n is the linear gain in the nth stage of the receiver.

The receiver noise figure is dominated by the noise figure of the front-end of the receiver if the gain of the front-end low-noise amplifier (LNA) is high. The components in the front end of the ACORDS receiver are tabulated below along with their respective noise figures and gain.

Stage N	**Component**	**Gain, G_n (dB)**	**Noise Figure, F_n (dB)**
1	Band Pass Filter	-0.5	0.5
2	Limiter	-0.3	0.3
3	SPDT switch	-1	1
4	Low Noise Amplifier	29	2

Table 3.2: Gain and noise figures of the components in the front end of the receiver

On substituting the above values into equation 3.5, the receiver noise figure is calculated to be 3.8 dB. Then substituting the noise figure into equation 3.4 will yield a system noise floor of about –97 dBm.

Signal processing gain

The digitized data are always pre-integrated before storage. The signal-to-noise ratio gain for N coherent integrations is N, while that for N incoherent integrations is $\sqrt{N}$ [10]. It is assumed that we would perform at least 1000 coherent integrations to obtain adequate sensitivity to sound 3-4 km of ice. This will lead to an integration gain (IG) of at least 30 dB ($10 * \log_{10}(1000)$).

Receiver gain

As the ACORDS receiver has two different channels, the gain in the various channels is derived as follows.

- Gain in the High Gain channel, (G_{HG})

The gain in the HG channel is the gain required to amplify the system noise floor to a level that is a 256 coherent-integration gain above the A/D noise level. It can be shown as follows:

$$N_{sys} + G_{HG} = P_{A/Dnoise} + IG \ ,$$

where IG is the integration gain

$$\begin{aligned} G_{HG}[dB] &= P_{A/Dnoise} + IG - N_{sys} \\ &= -63 + 30 - (-97) \\ &= 64dB \end{aligned} \quad . \qquad (3.6)$$

- Gain in the Low Gain (LG) channel, (G_{LG})

The gain in the LG channel is the maximum gain required to amplify the return from the air/ice interface to a signal level that does not saturate the A/D converter. It can be shown as follows

$$P_{i/p\max} + G_{LG} = P_{A/D\max} \quad , \tag{3.7}$$

where $P_{i/p\max}$ is the maximum received power from the air/ice interface

$$G_{LG}[dB] = P_{A/D\max} - P_{i/p\max}$$
$$= 4 - (-16.5) = 20.5dB \quad .$$

Therefore, the dual-channel receiver has been designed with a high gain of 80 dB and a low gain of 44 dB. Setting the digital attenuators accordingly in both the channels will reduce the gain.

3.2.2 Derivation of loop sensitivity

The minimum detectable signal (*MDS*) is a compression gain and a 1000 coherent-integration gain below the system noise floor. With no signal-to-noise ratio (*SNR*), this MDS can be given by

$$MDS\ [\text{dBm}] = N_{sys} - IG - CG + SNR \tag{3.8}$$

$$MDS = -97 - 30 - 16 + 0 \quad ,$$

$$MDS = -143\ \text{dBm}$$

where *CG* is the compression gain (10*log10 (*BT*)) and *T* is the uncompressed pulse width (2 μsec).

The loop sensitivity of the radar system is the ratio of the peak-transmit power to the *MDS*. As mentioned before, the peak-transmit power for the ACORDS is 200 Watts (53 dBm). Thus the loop sensitivity is given as

$$Sensitivity[dBm] = P_{peak} - MDS \tag{3.9}$$

$$= 53 - (-143) = 196 \text{ dB} \quad ,$$

where P_{peak} is the peak transmit power (53 dBm).

The loop sensitivity can be improved by either increasing the transmit power, reducing the system noise floor or increasing the compression gain.

3.3 Design process

3.3.1 Selection of WG and DAC clocks

According to the Nyquist theorem, the sampling frequency must be at least twice the maximum frequency of the signal. Hence the sampling frequency or clock of the D/A converter needs to be at least 320 MHz to generate a 140- to 160-MHz chirp signal. As there are not many off-the-shelf D/A converters that can operate at such high speeds, a bandpass sampling technique is used to generate the signal using clocks at lower speeds.

Oversampling [13] is a sampling technique that involves sampling a desired signal at a rate higher than the standard Nyquist rate. Bandpass sampling (undersampling) [14,15] is a technique that involves sampling a continuous bandpass signal at a rate lower than the standard Nyquist rate.

The ACORDS is a system that simultaneously oversamples and undersamples. The waveform generator in the digital system uses oversampling to generate a linear

140-160 MHz chirp from a linear baseband chirp. The data acquisition uses undersampling to directly digitize the RF return chirp at the output of the receiver. The fixed sampling frequencies that can be used for frequency translation without any aliasing can be calculated by the following equation [15]:

$$\frac{2f_l}{k-1} \geq f_s \geq \frac{2f_u}{k}$$
$$f_s \geq 2B \;\&\; 2 \leq k \leq \frac{f_u}{B}, \tag{3.10}$$

where f_l is the lower frequency (140 MHz), f_u is the higher frequency (160 MHz), B is the bandwidth of the band-pass signal (20 MHz), f_s is the eligible sampling frequency and k is a positive integer.

K	Range of f_s (MHz)
2	160.00 – 280.00
3	**106.67 - 140.00**
4	80.00 – 93.33
5	64.00 – 70.00
6	**53.33 - 56.00**
7	45.71 - 46.67

Table 3.3: Range of sampling frequencies for different values of k

The ranges of sampling frequencies for different values of k are tabulated above. The shape of the sampled signal spectrum will be flipped if k is even. We choose to select the oversampling frequency (f_{WG}) in the range of 106.67-140 MHz so that the desired chirp signal will be the first-order harmonic of the baseband chirp. We will thus need a 30- to 50-MHz baseband chirp digitized at 110 MHz in order to

generate a 140- to 160-MHz chirp signal. The concept of oversampling is shown in Figure 3.3.

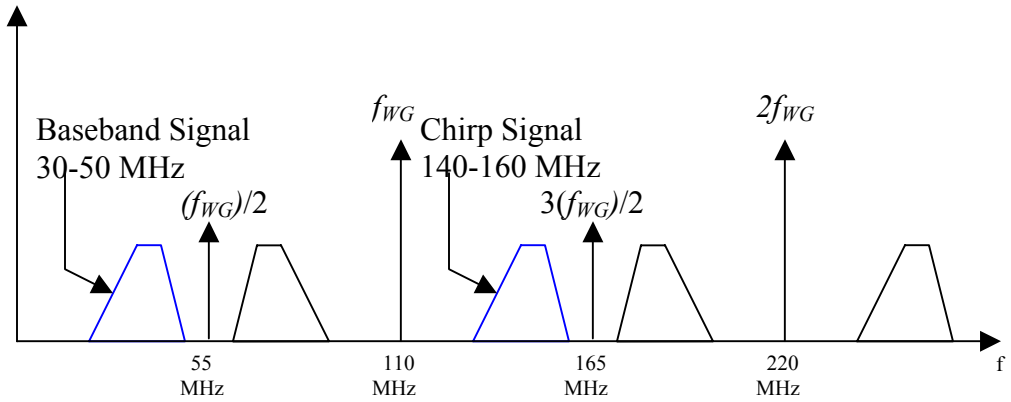

Figure 3.3: Oversampling concept

We selected the undersampling clock (f_{DAC}) as 55 MHz so that it can be derived easily from the oversampling clock. Thus the received chirp signal will be digitally translated down to the baseband (5-25 MHz). As k is even, the spectrum shape of the RF signal is flipped, but it can be compensated for in the signal processing. The concept of undersampling is shown in Figure 3.4.

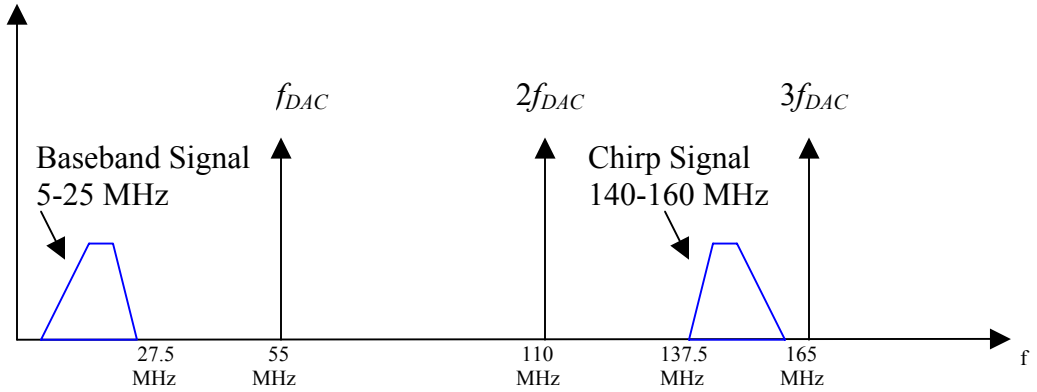

Figure 3.4: Undersampling concept

3.3.2 Digital pulse compression

Radar pulse compression can be implemented in either one of the analog or digital domains. It has been implemented in the analog domain in NG-CORDS. Analog pulse compression techniques use complementary SAW devices for both the signal generation and matched filtering of chirp waveforms. In the new system, digital design is used for signal generation, whereas the matched filtering is done digitally in the host computer.

The algorithm for the digital pulse compression [16] is shown in Figure 3.5. The received RF signal is first digitized in the data acquisition system at a rate of 55 MHz. The baseband chirp is then down converted to DC in a quadrature mixer. The sum signal and the higher-order harmonics are later filtered using a low-pass filter. An ideal baseband chirp sampled at the same rate is generated. The FFT process transforms both time-domain signals into the frequency domain. Matched filtering is achieved in the frequency domain when the spectra of the digitized and reference chirps are multiplied. The IFFT process of the multiplication gives the compressed baseband chirp with a pulse width of $1/B$.

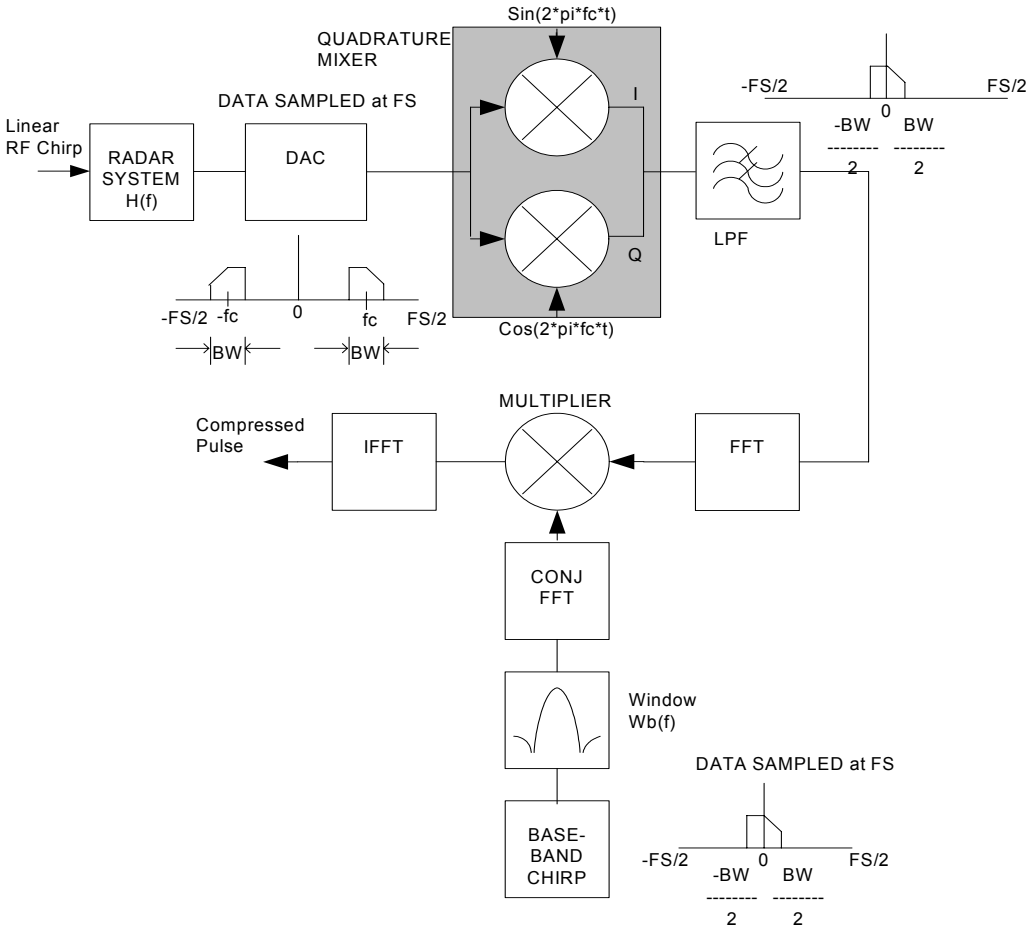

Figure 3.5: Digital pulse compression

3.4 Radar Transmitter

The ACORDS transmitter has been completely redesigned. In the NG-CORDS transmitter, a Surface Acoustic Wave (SAW) expander is used to generate the chirp pulse. The main part of the ACORDS transmitter is a Waveform Generator (WG) that is used to generate the chirp pulse. This chirp is then filtered and amplified before it is transmitted.

In the next section, a description of the WG will be given. The following sections will deal with the design of the transmitter, its construction and housing.

3.4.1 Waveform Generator

A detailed description of the WG is given in Tammana [12]; thus only a brief description of the WG is given here. The WG is a programmable waveform generator that generates a desired waveform. A sampled and digitized waveform is loaded into the WG. The WG sequentially reads and stores these values into a memory before sending them into a digital-to-analog (D/A) converter. The D/A converter then generates the desired waveform.

The AD9777 D/A converter from Analog Devices is used in the WG. The AD9777 is an interpolating TxDAC with 16-bit resolution. The WG digitizes a baseband chirp using an oversampling clock of 110 MHz. The 140- to 160-MHz chirp signal is derived from the baseband chirp by selecting the first harmonic image of the baseband chirp. The interpolator in the AD9777 is set to double the input data rate. The data are then passed through a high-pass filter. The filtered data are internally

modulated by $F_{DAC}/2$ to create the mirror images. The amplitude of these images rolls off according to

$$\frac{\sin \pi(F_{out} / F_{DAC})}{\pi(F_{out} / F_{DAC})} \quad , \tag{3.11}$$

where F_{out} is the fundamental output frequency and F_{DAC} is the interpolated sampling clock to the D/A converter.

The harmonic analysis of the AD9777 is shown in Figure 3.6. The harmonic images and the spurious signals for a single frequency output (40 MHz) from AD9777 are shown in red and blue, respectively. The high-pass filter suppresses the fundamental output and hence the output of the TxDAC contains only the images. A bandpass reconstruction filter is used at the output of the WG to select the harmonic at 150MHz ($F_{DAC}/2 + F_{fund}$). The chirp signal at the output of the WG is at –7 dBm.

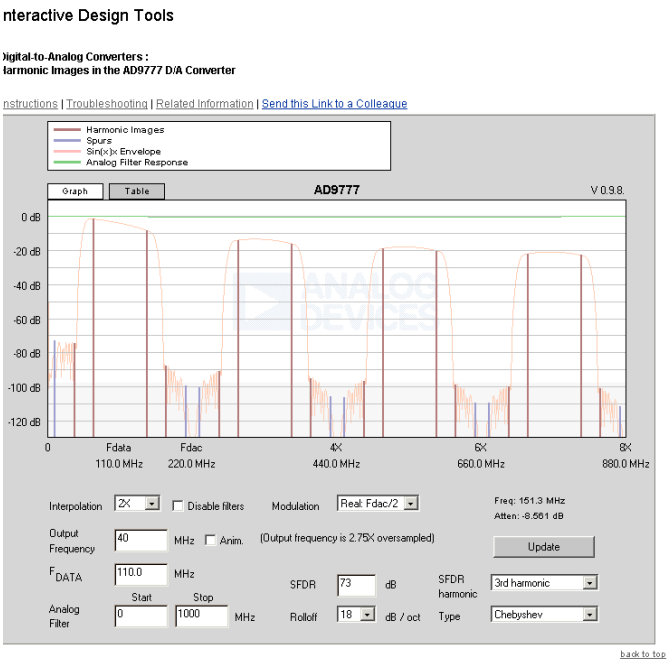

Figure 3.6: Harmonic analysis of the AD9777

3.4.2 Transmitter design

The transmitter consists of an RF section and a clock synchronization section. The RF section contains RFICs to filter and amplify the generated chirp signal. The clock synchronization section generates the required clocks for the WG and the data acquisition module.

3.4.2.1 RF section design

The WG generates a linear 140- to 160-MHz chirp at –7 dBm. The main purpose of the RF section is to amplify the chirp signal to a 200-W peak power level. Figure 3.7 shows the block diagram of the transmitter's RF section. All the components in the shaded portion of the block diagram are surface-mount type. The part number and the specifications are listed below each component.

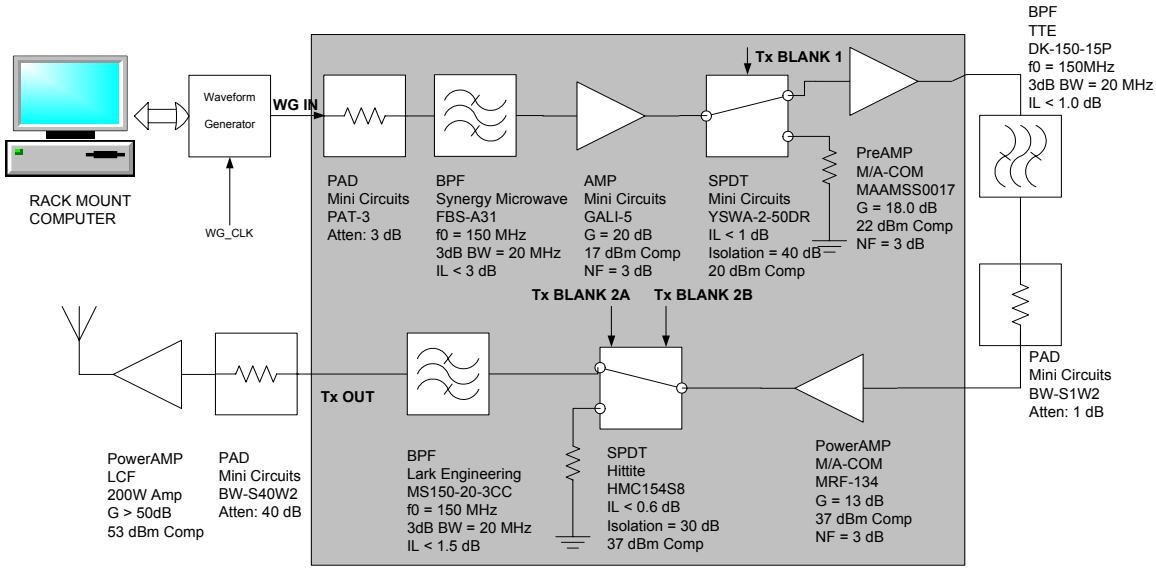

Figure 3.7: Block diagram of the RF section of the ACORDS transmitter

As mentioned above, the WG generates a linear chirp at –7 dBm peak power. A 3-dB pad attenuates the output of the WG. This attenuator not only serves to reduce

any reflections but also to adjust the power level so as to prevent saturation. A bandpass filter (BPF) with good stopband attenuation is inserted to filter the harmonics and spurious signals generated by the WG. The amplifier following the BPF is one of the four amplifiers used to amplify the chirp pulse to a peak power of 200 W. An absorptive GaAs switch with internal TTL drivers is then inserted. This switch is controlled by a blanking signal (Tx BLANK 1). It serves as a transmitter ON/OFF switch and also reduces the time-sidelobes and transmitter leakage power. This switch is set to turn on and off at the leading and trailing edges of the chirped pulse, thereby creating a neat rectangular shape pulse. The amplifier, a GaAs MMIC, following the low-power switch pre-amplifies the chirp pulse before it is fed to the power amplifier. A BPF with low insertion loss is inserted to filter out any harmonics if present. The amplifiers and switch following the BPF are high-power components.

The high-power switch and amplifier used in the NG-CORDS transmitter have been replaced in the ACORDS transmitter design. An M/A-COM MRF134 Field-Effect Transistor (MOSFET) replaced the Motorola CA2832C wideband, linear amplifier. Figure 3.8 shows the schematic of the 2-W power amplifier circuit used in the radar. As small-signal S parameters cannot be applied to power amplifier design, large-signal impedance data provided in the data sheet were used to design the matching networks. Stability is achieved by using a 68-ohm input shunt-loading resistor. The gain of the power transistor can be changed by tuning the four variable capacitors present in the schematic. The gate bias voltage is regulated from 5 V using

an adjustable voltage regulator. The power transistor was tested individually before being included in the final design.

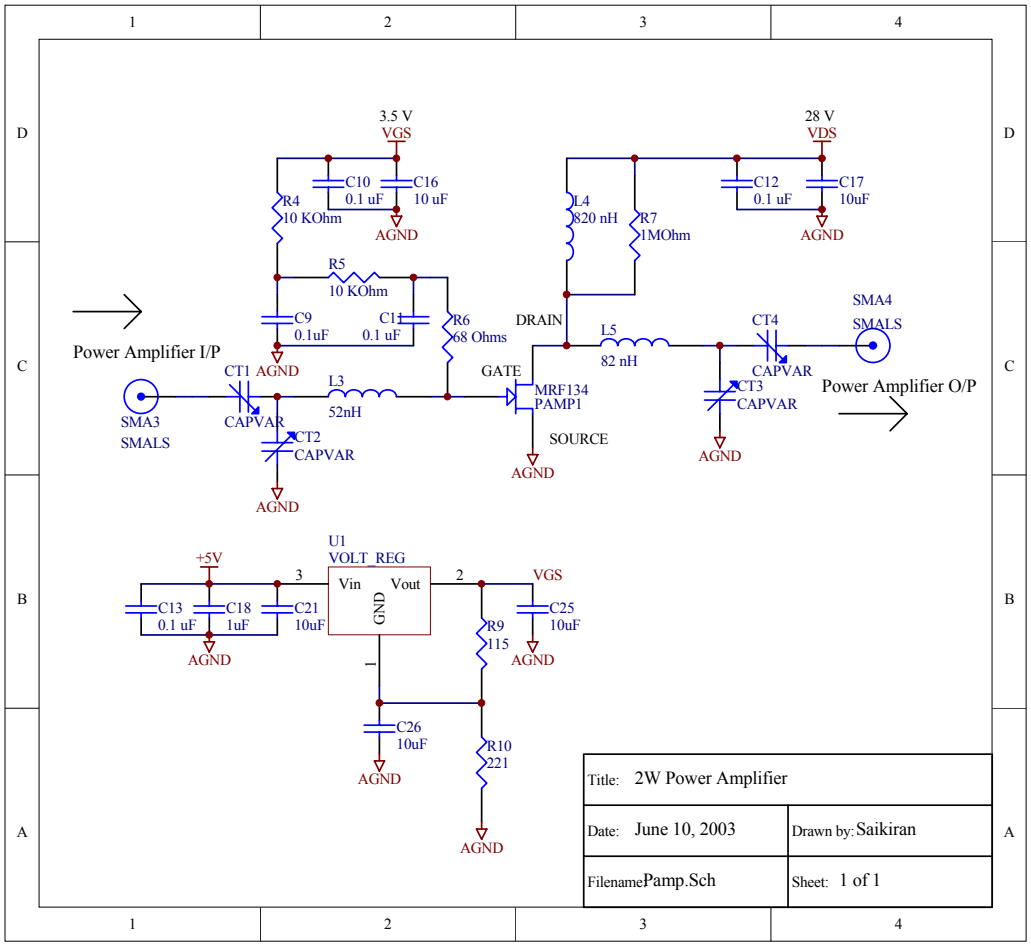

Figure 3.8: Schematic of the 2-W power amplifier

A Hittite HMC154S8 switch that has its own internal TTL drivers has replaced the high-power switch in the NG-CORDS transmitter. This switch is controlled by a set of complementary blanking signals (Tx BLANK 2A and 2B). It can handle RF power up to 5 W and further reduces the range-sidelobes and transmitter leakage power. Following the high-power switch is a BPF with very low insertion loss and power handling capabilities up to 20 W. The purpose of the BPF is

to filter the harmonics generated by the power amplifier. An off-the-shelf power amplifier from LCF is used to further amplify the chirp signal to a peak power of 200 W.

3.4.2.2 Clock synchronization design

The clock section generates all the clocks required for the digital system. The schematic of the synchronization circuit is shown in Figure 3.9. It contains a Temperature Controlled Crystal Oscillator (TCXO) that generates a stable, 10MHz TTL signal. The output of the oscillator is fed to a two-way power splitter. The output

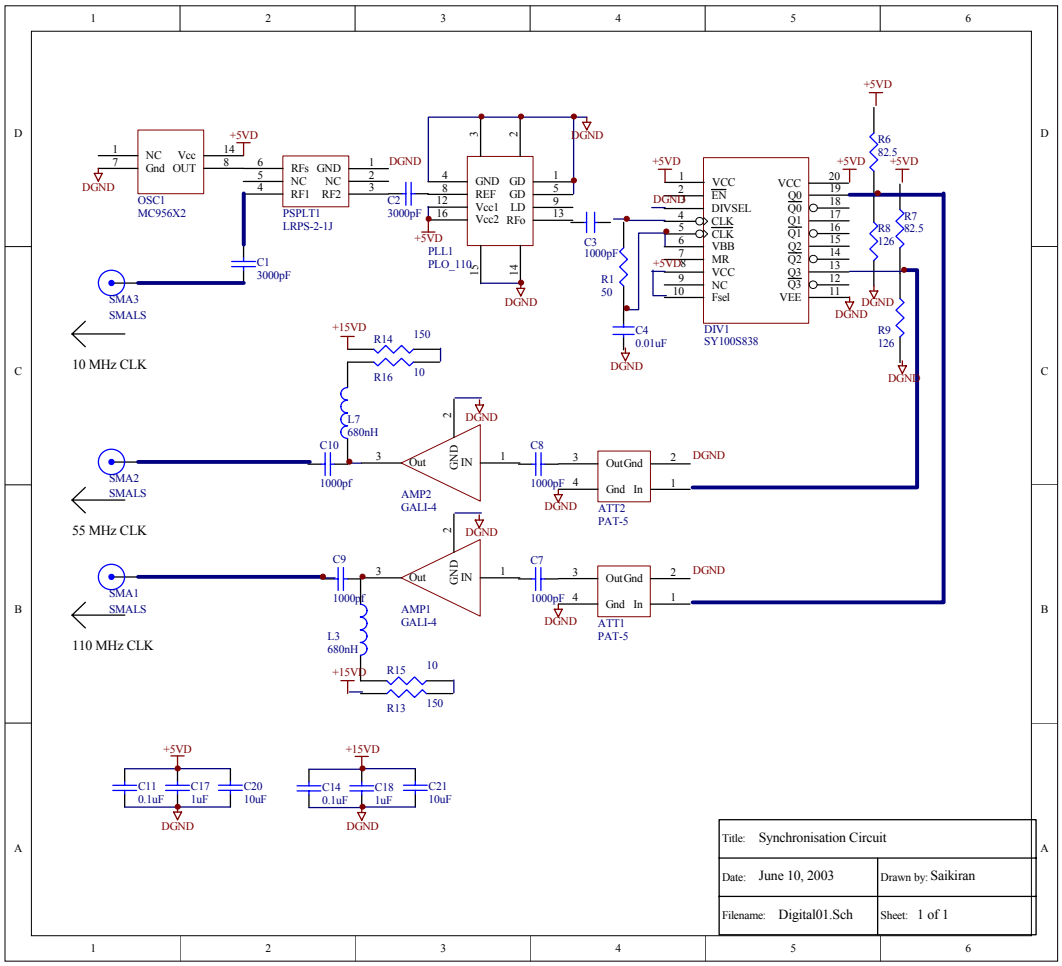

Figure 3.9: Schematic of the synchronization circuit

from one port is used to generate the 110-MHz and 55-MHz clocks, whereas the other output is low pass filtered to generate a clean 10-MHz CW wave. To generate the other clocks, the output of port1 is fed to a fixed-frequency phase- locked oscillator (PLO) with good phase noise performance. The PLO has a built-in PLL circuit to generate a 110-MHz CW signal from a 10-MHz input. Following the PLO is Positive Emitter Couple Logic (PECL) clock divider chip that generates the 55-MHz signal. The clock divider chip functions as a divide by 1 and divide by 2 chip when the Fsel and DIVSEL pins are set accordingly. The 110-MHz CW signal drives the divider chip by using the V_{BB} voltage provided by the chip itself. The circuitry following each output of the PECL chip consists of a pad and an amplifier. The pads are inserted to prevent the amplifier from saturation, whereas the amplifier is included to boost the output levels of the PECL signals.

3.4.3 Transmitter construction

The ACORDS transmitter consists of two sections, namely the RF section and the clock synchronization section. The RF section is designed using microwave techniques on a two-layered 3.6'' x 5.6'' FR4 board. The clock synchronization section is designed on a two-layered 2.6'' x 3.6'' FR4 board. The schematic and printed circuit board (PCB) layout were created using Protel's EDA Client [17]. The top layer contains the signal lines, whereas the bottom layer contains few power lines. These PCBs have been fabricated outside and have a solder mask protection. The PCB layouts for the RF and clock synchronization section are shown in Figures 3.10 and 3.11 respectively.

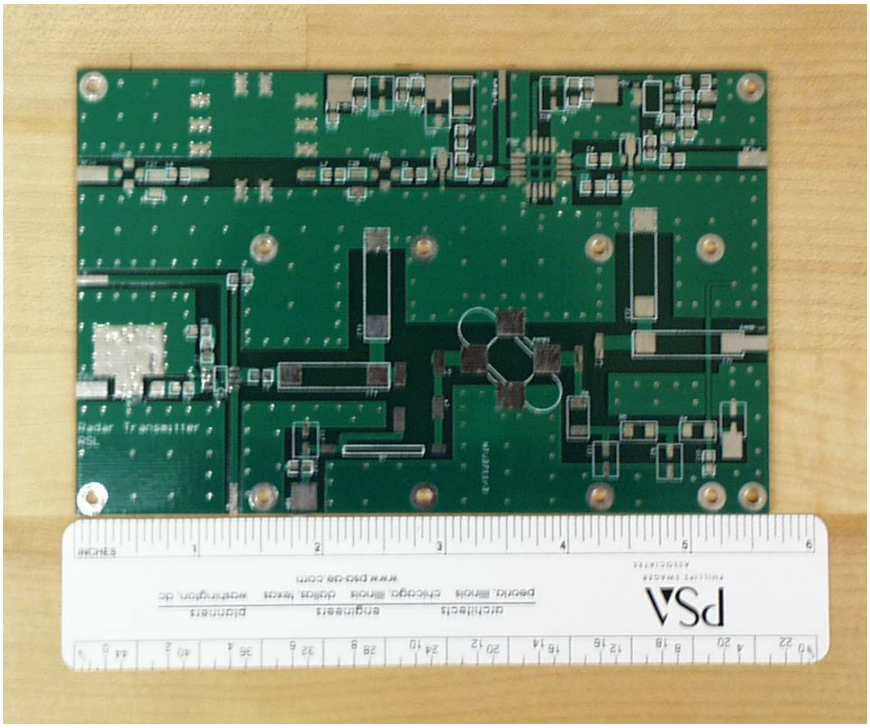

Figure 3.10: Photograph of the PCB layout of the RF section before populating parts

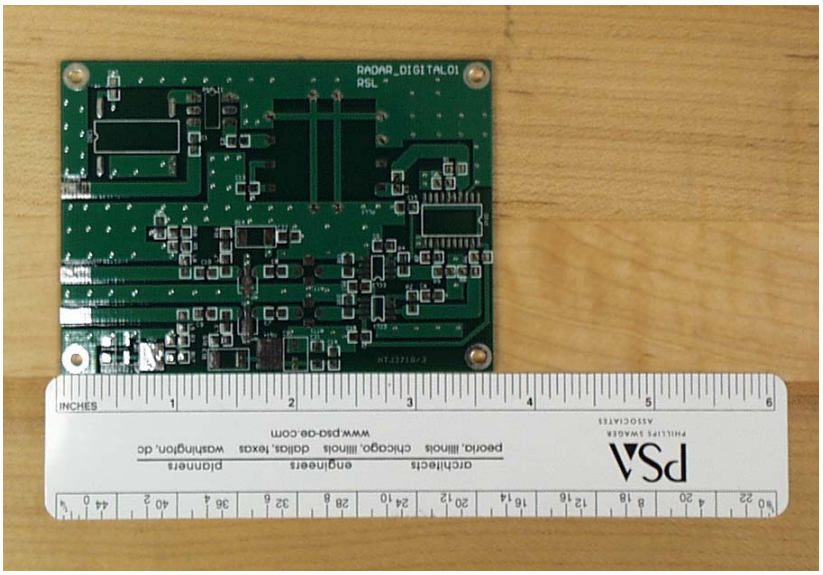

Figure 3.11: Photograph of the PCB layout of the clock synchronization section before populating parts

After the components were populated, each section was tested individually. Each board was then packaged in an RF shielded enclosure. These enclosures were

purchased rather than built, as they are inexpensive and come in many standard sizes. They have RF shielding capabilities to 60 dB up to 3 GHz. The RF section and clock section of the transmitter were designed so that they could fit in a standard RF enclosure. The RF section is packaged in a 4'' x 6'' enclosure, whereas the clock section is fit into a 3'' x 4'' enclosure. These packaged enclosures will be referred to as modules.

Figure 3.12 shows the photograph of the transmitter RF module. SMA connectors are used to extend control and RF signals to outside the enclosure, whereas RFI feed-through filters are used to extend the power lines. These filters are low-pass filters that attenuate any signals other than DC by at least 40 dB [18]. The MOSFET power transistor used in the transmitter has a different flange-mount package. To place the transistor on the board, a part of the FR4 board had to be milled out. As the transistor generates a lot of heat, a 1.25'' x 2'' x 0.5'' aluminum block is used to sink the heat generated. This heat sink connects the analog ground on the board to the bottom plate of the RF enclosure. In addition to the heat sink, standoffs are used for grounding. The control ports are shown in red, whereas the RF ports are shown in black. The three control signals required for the switches in the transmitter are generated by the digital system.

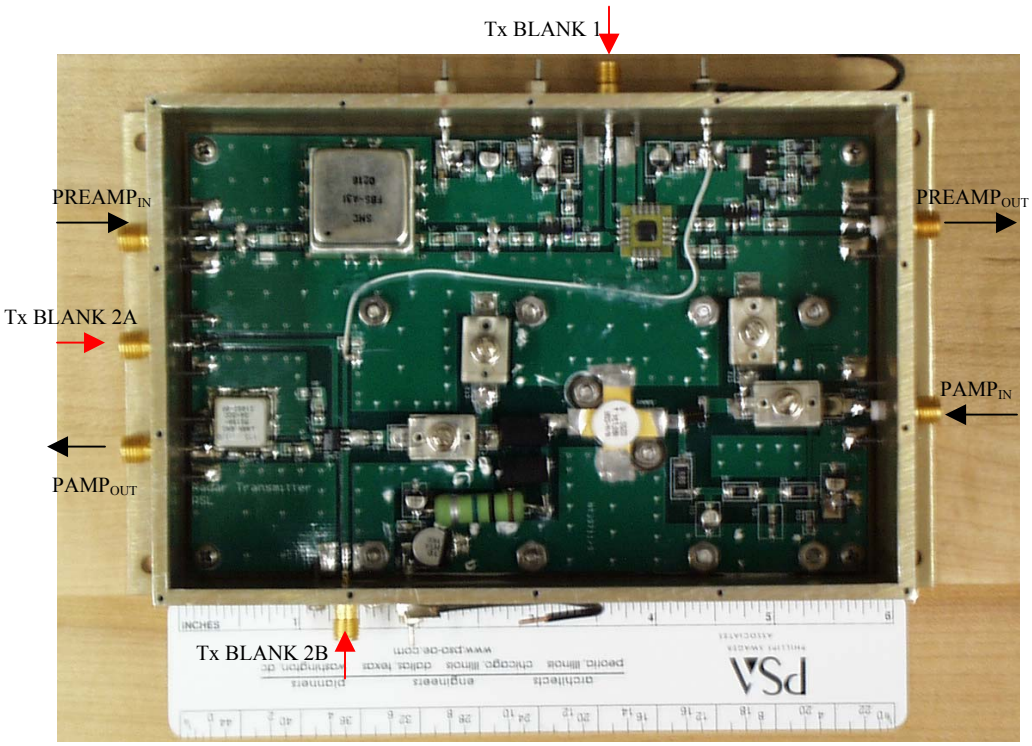

Figure 3.12: Photograph of the transmitter RF module

The clock synchronization module has been constructed similarly to the RF module and is as shown in Figure 3.13. This module is a digital circuit and does not generate much heat. Hence instead of a heat sink, standoffs are used to connect the digital ground to the base plate of the enclosure. The respective signal ports are shown in black.

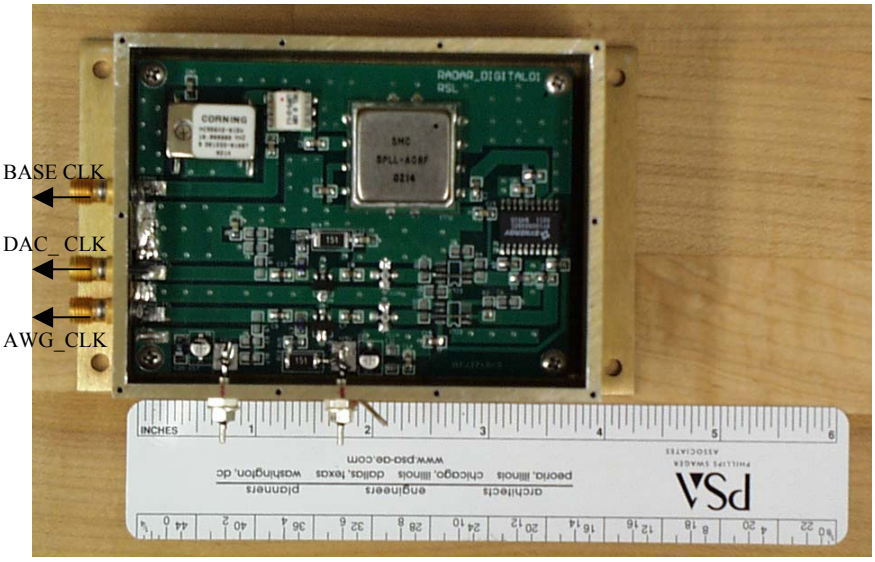

Figure 3.13: Photograph of the clock synchronization module

In addition to the above modules, the transmitter has only two other connectorized components. The first one is a bandpass filter and is present between the $PREAMP_{IN}$ and $PAMP_{OUT}$ ports of the RF module. The second one is a low pass filter with a 15-MHz cutoff and is present at the BASE CLK port of the clock synchronization module.

3.5 Dual-Channel Receiver

The ACORDS receiver has been completely redesigned. Compared to the NG-CORDS receiver, the ACORDS receiver has many improvements. The improvements are listed as follows:

- Low Gain (LG) and High Gain (HG) instead of I and Q channels
- No sensitivity time control to prevent the receiver from saturation
- Receiver gain controlled by digital attenuators instead of an analog attenuator
- No analog down conversion

In the next section, a description of the dual channel receiver will be given. The following section will deal with its construction and housing.

3.5.1 Dual-channel receiver design

The receiver consists of an RF section. There is no intermediate frequency (IF) section as the down conversion from bandpass to baseband is done in the data acquisition module. The RF section contains RFICs to filter and amplify the return echoes.

3.5.1.1 RF section design

The main purpose of the RF section is to amplify the weak returns from the bedrock. Figure 3.14 shows the block diagram of the RF section of the receiver. All the components in the shaded portion of the block diagram are surface-mount type. The part number and the specifications are listed below each component.

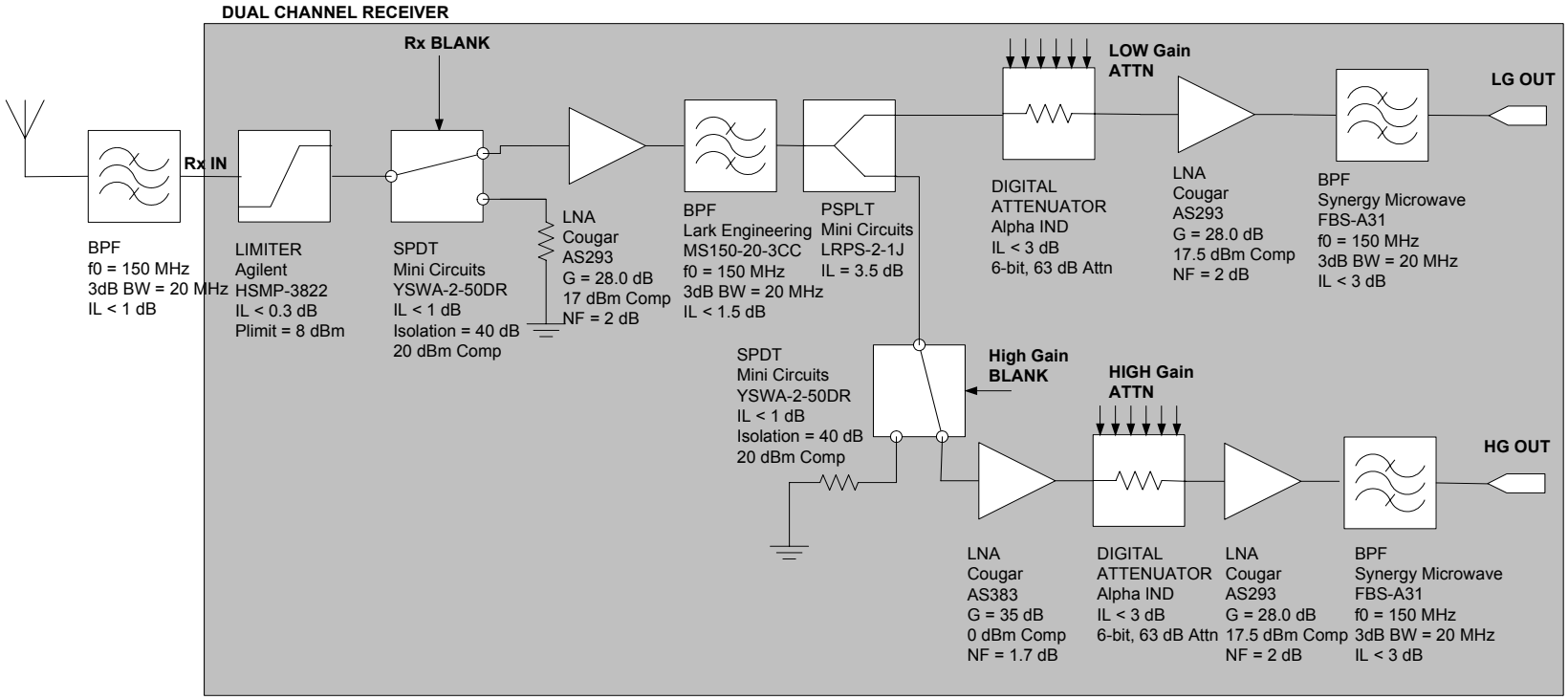

Figure 3.14: Block diagram of the RF section of the ACORDS receiver

The echo signals from the ice are received through the receive dipole array. The front end of the receiver contains a BPF, limiter, switch and a LNA. The BPF used is an SMA-connectorized component with a very low insertion loss and is used to filter the out-of-band signals. A limiter, following the BPF, protects the receiver from strong echoes. The Watkin Johnson limiter used in the NG-CORDS receiver is a passive component but has 1-dB insertion loss. We wanted to replace it with a very low insertion loss limiter to improve the noise figure of the receiver. Hence, a limiter diode with 0.3 dB insertion loss has been used. A receiver-blanking switch is used to turn the receiver off when the radar is transmitting. The NG-CORDS receiver used a YSWA-2-50DR absorptive switch from Mini Circuits to function as a blanking switch. We used the same part as it is inexpensive and provides at least 40 dB attenuation.

An LNA with a low noise figure has to be used for the amplification in the first stage. We could not use the NG-CORDS LNA as it has become obsolete. We wanted to use an LNA with a low noise figure and a high 1-dB compression point. We found two RFIC LNAs that suit our requirements. The AS293 from Cougar Components has a noise figure of 2 dB and a 1-dB compression point of 16 dBm, whereas the AFSM2-00100200-12-8P from Miteq has a noise figure of 1.2 dB and a 1-dB compression point of 8 dBm. Even though the latter one has a lower noise figure, we decided to use the LNA from Cougar, as it is less expensive and has a higher 1-dB compression point. As this amplifier has enough gain, we used it for subsequent amplifier stages.

A BPF filter with a low-insertion loss is inserted to filter harmonics. Following the filter is a power splitter that splits the return echo equally into two different channels. The Low Gain (LG) channel has less gain, whereas the High Gain (HG) channel has more gain. In the LG channel a digital attenuator is placed before the LNA. The attenuation is controlled digitally and it prevents saturation of the LNA in the final stage. The digital attenuator consists of two individual low-cost GaAs ICs from Alpha IND. The AA260-85 is a 5-bit attenuator with 31 dB total attenuation in steps of 1 dB. The AA104-73 is a 1-bit attenuator with 32 dB attenuation in a single step. These two ICs when combined yield a 6-bit, 63 dB total attenuation in steps of 1 dB. The last BPF in the LG channel is an anti-aliasing filter with high stop band attenuation.

The HG channel is similar to the LG channel except for an additional LNA and a Mini Circuits switch that is included. The functionality of this switch is to protect the HG channel of the receiver from saturation. This switch is blanked (OFF state) to attenuate the strong returns from the air/ice interface and few internal layers. It does not affect the weak returns from the bedrock. We have selected the Cougar AS383 LNA to provide the additional gain in this channel. The two channel outputs from the receiver are then sent to the data acquisition module where they are digitized, integrated and stored.

3.5.2 Receiver construction and housing

The ACORDS receiver consists of an RF section only. The RF section has been designed using microwave techniques on a two-layered 3.6'' x 5.6'' FR4 board.

The top layer contains the signal lines, whereas the bottom layer contains a few power lines and control lines for the digital attenuator. The PCB for the RF section is shown in Figure 3.15.

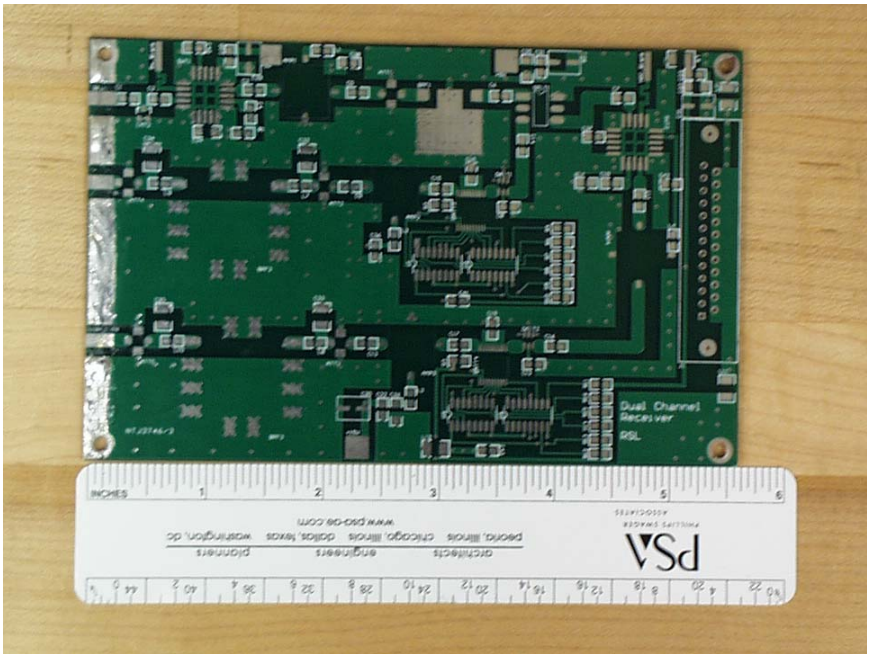

Figure 3.15: Photograph of the PCB layout of the RF section before populating parts

The construction of the receiver module was done in stages, similar to that of the transmitter. The RF board was populated, tested individually and then housed in a 4'' x 6'' RF enclosure. Figure 3.16 shows the photograph of the receiver RF module. SMA connectors are used to extend control and RF signals to outside the enclosure, whereas RFI feed-through filters are used to extend the power lines. These filters are low-pass filters that attenuate any signal other than DC by at least 40 dB [18]. A 25-pin D-type connector is used to provide the digital attenuator bits to both the channels. The pin assignment of the 25-pin connector is shown in Table 3.4.

Pin No.	Assignment	Pin No.	Assignment
1	HG 32 dB	8	LG 16 dB
2	HG 16 dB	9	LG 8 dB
3	HG 8 dB	10	LG 4 dB
4	HG 4 dB	11	LG 2 dB
5	HG 2 dB	12	LG 1 dB
6	HG 1 dB	13	NC
7	LG 32 dB	14 - 25	Digital ground

Table 3.4: Pin assignment of the 25-pin D-type connector

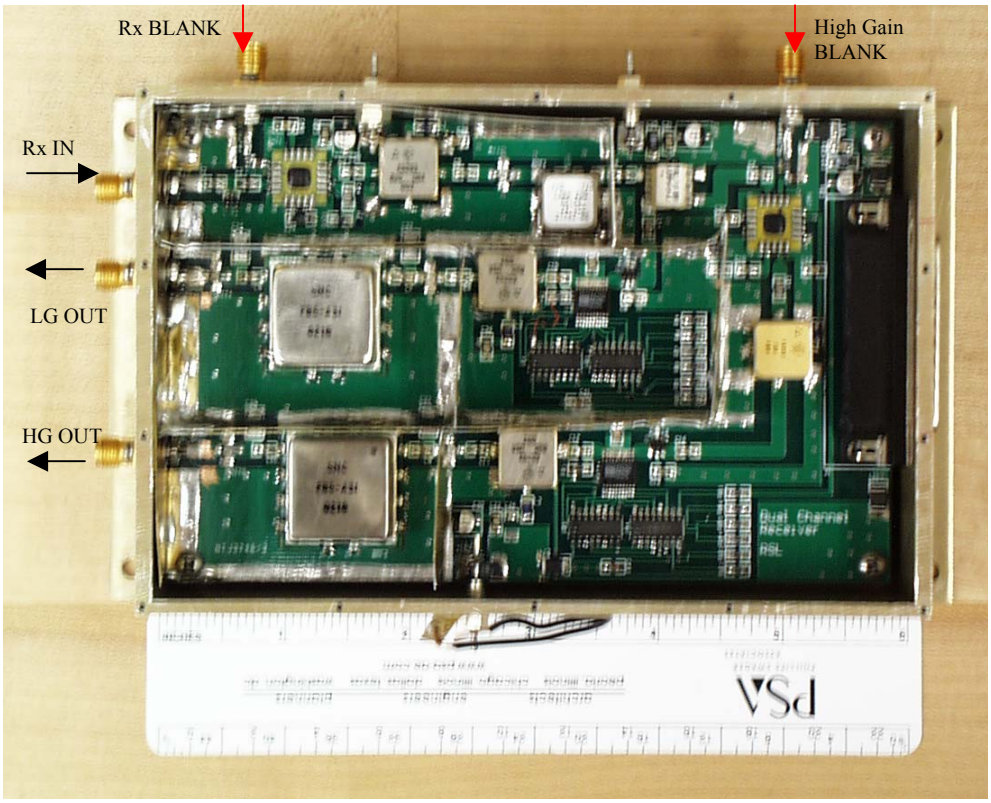

Figure 3.16: Photograph of the receiver RF module

Coupling of any undesired signals into the front end of the receiver module would cause oscillations. Standard RF shields are used to isolate the front end of the

receiver from the LG channel and the HG channel and thus prevent oscillations. RF shields are also inserted between the LG and HG sections.

As the receiver is a low-noise and high gain receiver, noise reduction techniques [19] are used in the construction of the receiver. Decoupling capacitors are placed as close as possible to IC power supply pins. Ground planes are placed close to the RF lines. These ground planes are connected to the other side of the circuit board using plated-through holes. As these boards were given out for fabrication, we used at least 15 plated-through holes per square inch to reduce lead inductance.

3.6 ACORDS digital system

The NG-CORDS digital system [5] was built in 1997. It uses 12-bit A/D converters and is compatible with a Pentium-based PC. It uses an ISA and a PCI card. The digital system was used in the field experiments from 1998 to 2002. Some of the disadvantages of the previous digital system were as follows:

- Control signals generated by triggering sections present in the radar system.
- Transmit waveform generated by SAW expander

A new digital system has been built to eliminate the above problems. The ACORDS digital system has been designed and developed by Torry Akins. It consists of three modules, namely 1) Waveform Generator (WG), 2) Data Acquisition, and 3) Triggering section.

The WG module is briefly explained in section 3.4.1. The data acquisition module consists of two channels. Each channel uses 12-bit A/D converters with high input bandwidth. The A/Ds are selected such that they can undersample the LG and

HG channels at a maximum sampling rate of 65 MSPS. The triggering section generates all the control signals required by the radar system. It also sets the attenuation in the digital attenuators. The advantages of the ACORDS digital system over the NG-CORDS digital system are as follows:

- Digital chirp waveform generation
- Undersampling of LG and HG channels
- Switches and attenuators in the radar system controlled digitally

The Graphical User Interface (GUI) for the digital system has been developed in C++. The GUI has real-time gray scale display of the LG and HG channels as well as the pulse-compressed signals. Radar parameters such as the transmit pulse width and transmit weighting function are set in the GUI. The duration of the control pulse for the Rx and HG blanking signals can be changed in the GUI itself. The attenuation values for the digital attenuators in the receiver are also set here.

The ACORDS digital system is housed in a 17'' x 17'' x 7.5'' rack-mountable chassis. Figure 3.17 shows the photograph of the digital system. The digital system is connected to the host computer through a standard Universal Serial Bus (USB) port. A 36-line ribbon cable is used as an interface between the digital system and the analog system. The control signals and the attenuator bits are sent to the radar system through this cable.

Figure 3.17: Digital system of the ACORDS

3.7 Analog system housing

The analog system of the ACORDS includes a triple-output (+15 V, +5 V, -5 V) linear power supply with current ratings of 3A, 10A and 1.5A respectively; +28V linear power supply with 1.5A current rating; transmitter RF module; receiver RF module; clock synchronization module; and interface card. All these are integrated in an 18'' x 24'' x 7'' rack mount chassis. Figure 3.18 shows the ACORDS analog system, whereas Figure 3.19 shows the front view of the analog system.

The interface card is mounted through the front panel of the chassis. The purpose of the interface card is to buffer and replicate the control signals and attenuator bits coming from the digital system. The control signals in the first set are internally routed to their respective ports using a twisted-pair wire, whereas the second set is brought out of the chassis through SMA feed-through bulkhead

connectors. Similarly, one set of the attenuator bits is internally routed to the 25-pin DB connector. LEDs are used in the front panel to indicate the attenuation set in the LG and HG channels. Table 3.5 shows the routing of the pin set on the interface card.

Description	Pin Set (0-31)	Front Panel Type	Internal routing
Waveform Generator Trigger	0	SMA	Not Used
Data Acquisition Trigger	1	SMA	Not Used
Tx Blank1	2	SMA	Tx Blank1
Tx Blank2A	3	SMA	Tx Blank2A
Tx Blank2B	4	SMA	Tx Blank2B
Receiver Blanking	5	SMA	Rx Blank
High Gain Blanking	6	SMA	High Gain Blank
Low Gain Atten	13-8	LEDs	7-12 *
High Gain Atten.	19-14	LEDs	1-6 *

Table 3.5: Routing of the pin set on the interface card
* 25-pin DB connections in the receiver RF module

In addition to the control signals, the eight signal ports-- Base CLK, WG CLK, DAC CLK, Tx OUT, WG IN, Rx IN, LG OUT and HG OUT--are brought out of the front panel using SMA feed-through bulkhead connectors. Minibend cables [20] are used to connect the RF ports, whereas shielded twisted-pair wires are used for power connections. The ground tabs on the individual modules are interconnected electrically. The modules are also bolted to the bottom plate and thus the chassis acts as a common electrical ground.

A four-inch diameter fan is mounted on the back panel of the chassis for cooling purposes. A switch on the front panel enables power control of the analog system. An LED is also mounted on the front panel to indicate the functionality of the power supply.

Figure 3.18: Analog system of the ACORDS

Figure 3.19: Front view of the analog system

3.8 Laboratory test results of the ACORDS system

The ACORDS system was tested in the laboratory. The digital system was programmed to generate a 2-μs–wide 140-160 MHz chirp signal. The attenuation in both the gain channels was set to 8 dB. The Rx Blank and the High Gain Blank signals were set to be ON. The BASE_CLK, WG_CLK and DAC_CLK clock signals as seen on an oscilloscope are shown in Figure 3.20. The 2-W RF chirp signal, at the output of a 20-dB attenuator, digitized by an oscilloscope is shown in Figure 3.21. The amplitude distortions in the 2-W RF chirp are caused by the non-linearities in the power transistor.

Before the dual channel receiver was tested with the data acquisition module, it was tested for its noise level. The Rx IN port was terminated with a 50 Ω load and the LG OUT, HG OUT ports were connected to an oscilloscope. The noise level measured at the LG OUT and HG OUT ports were –59 dBm and –26 dBm respectively.

The sidelobe performance of the ACORDS was evaluated by performing a loop-back test. The experimental setup for a loop-back test of the ACORDS is shown in Figure 3.22. The LCF power amplifier amplified the 2-W chirp signal to a peak power of 200 W. A fiber optic delay line [21] was used to simulate the air/ice interface. The delay line was used to delay the transmitted chirp signal by 10 usec. The attenuation in the delay line is set at 69 dB. The delayed output was connected to the Rx IN port of the receiver through a 70-dB attenuator.

Figure 3.23 shows the digitized, unweighted and undersampled LG and HG chirp signals, whereas Figure 3.24 shows the compression results. The direct chirp and the system feed-through that are barely seen in the LG channel (Figure 3.23) show up after the pulse compression (Figure 3.24). The signals at either side of the compressed pulse are the range sidelobes and are 16 dBc below the main pulse.

As mentioned before, weighting can be applied either to the transmit chirp or to the ideal baseband chirp to reduce sidelobes. We reprogrammed the digital system to weight the transmit chirp by a Hamming function. The zoomed-in compression result for the HG chirp with different weightings is shown in Figure 3.25. The sidelobe performance is best for the case when both the transmit chirp and the ideal baseband chirp are Hamming weighted. The first range sidelobe on the left side of the main pulse is 35 dBc below the main pulse.

It can be seen in Figure 3.25 that the Hamming weighting applied did not achieve the specified sidelobes. In order to verify the performance, we simulated an ideal chirp with a time-bandwidth (*BT*) product of 40 and compressed it with itself. It was assumed that the system is ideal. The compression result for an ideal chirp with different weightings is shown in Figure 3.26. Distant range sidelobes can be seen for the case where the baseband chirp was Hamming weighted.

The sidelobe performance in Figures 3.25 and 3.26 can be attributed to two factors, namely 1) small time-bandwidth (*BT*) product, and 2) system transfer function. It has been reported that weighting achieves the specified sidelobes for large *BT* (> 60) products only. In the case of small *BT* products, the compressed output

contains a pair of distant sidelobes placed at +/- *T/2* with respect to the main lobe. The distant sidelobes, also known as paired-echo or distortion sidelobes, are caused by the Fresnel ripples present in the amplitude spectrum [22, 23]. They are caused due to the deviation of the frequency spectrum from an ideal rectangular spectrum.

It can be seen from Figures 3.25 and 3.26 that amplitude weighting of both the transmit and baseband signals has reduced the distortion sidelobes. In this case the weighting of the transmit chirp has reduced the amplitude ripples in the frequency spectrum. Hence it was decided to apply Hamming weighting on both the transmit and baseband chirps.

Phase predistortion is a different method used to reduce the distortion sidelobes. It has been shown that a predistorted FM chirp with amplitude or phase shaping reduces the spectrum ripple and its associated paired-echo sidelobes [23]. A predistorted chirp can be considered as the sum of three independent FM chirp signals with each segment having different phase modulation. We simulated the compressed pulse for a predistorted chirp and compared its sidelobe performance with that of an ideal chirp. Figure 3.27 compares the FM function and the amplitude spectrum of the predistorted chirp with that of an ideal chirp. It can be seen that the spectrum ripples in the predistorted chirp are smaller. Figure 3.28 shows the compression result of an ideal and predistorted chirp for a Hamming window. It can be seen that the distant range sidelobes have been reduced in the predistorted case. A better predistortion function can be designed to achieve low sidelobes.

The practical loop sensitivity of the ACORDS is the sum of the signal-to-noise (SNR) after 1000 coherent integrations and pulse compression with the delay-line attenuation (69 dB) and the input padding (70 dB) at the receiver. It can be seen from Figure 3.24 that the measured SNR is around 55 dB. The practical loop sensitivity of the ACORDS is calculated to be around 194 dB.

The sidelobe performance in the ACORDS system has been improved by 9 dB. The measured loop sensitivity is only 1 dB better than that of the NG-CORDS system. The field experiment results of the ACORDS system are discussed in the next chapter. The sidelobe performance can be improved further by amplitude and phase modulating the chirp signal generated by the arbitrary waveform generator to reduce distortion associated with low BT product. Also, ampltidue and phase distortion introduced by the power amplifier can be compensated for with the arbitrary waveform generator. Because the system was shipped immediately after integrating the RF and digital systems, we did not have an opportunity to implement ripple distortion and power amplifier compensation in the chirp signal.

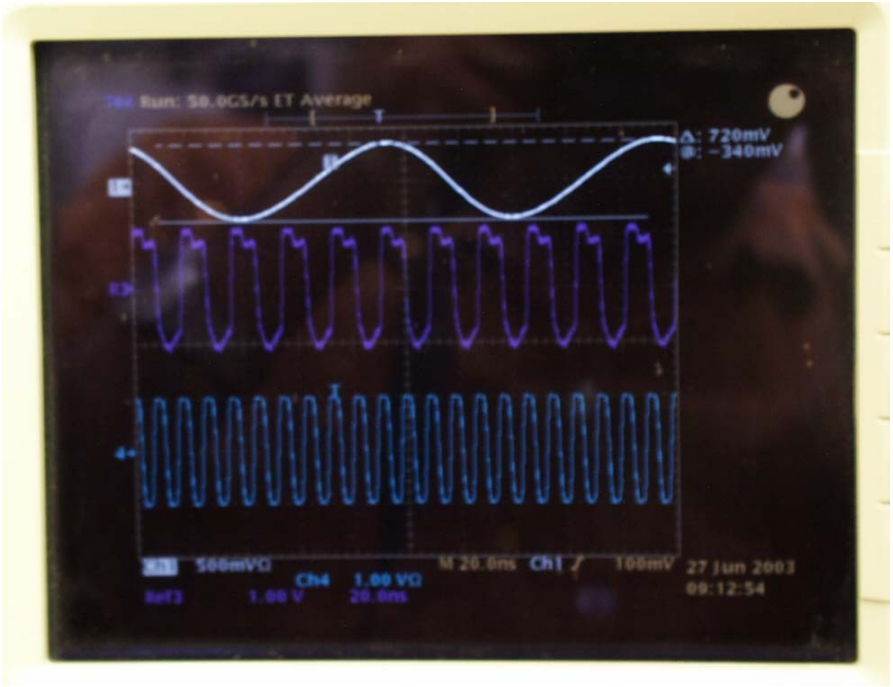

Figure 3.20: Oscilloscope display of BASE_CLK (top), DAC_CLK (middle) and WG_CLK (bottom)

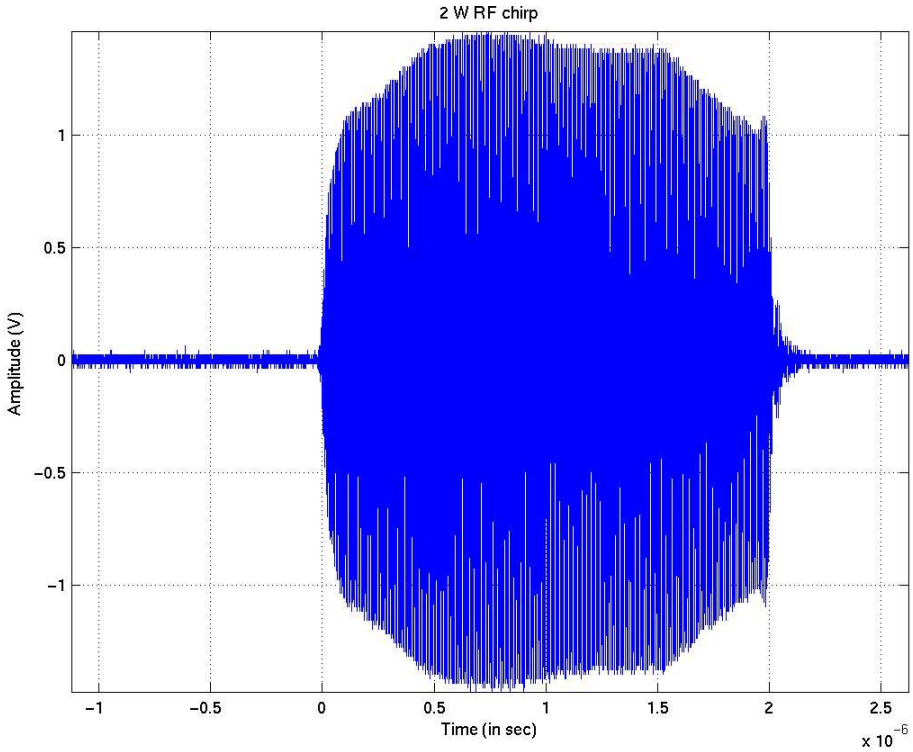

Figure 3.21: Digitized 2 W RF chirp signal after 20 dB attenuation

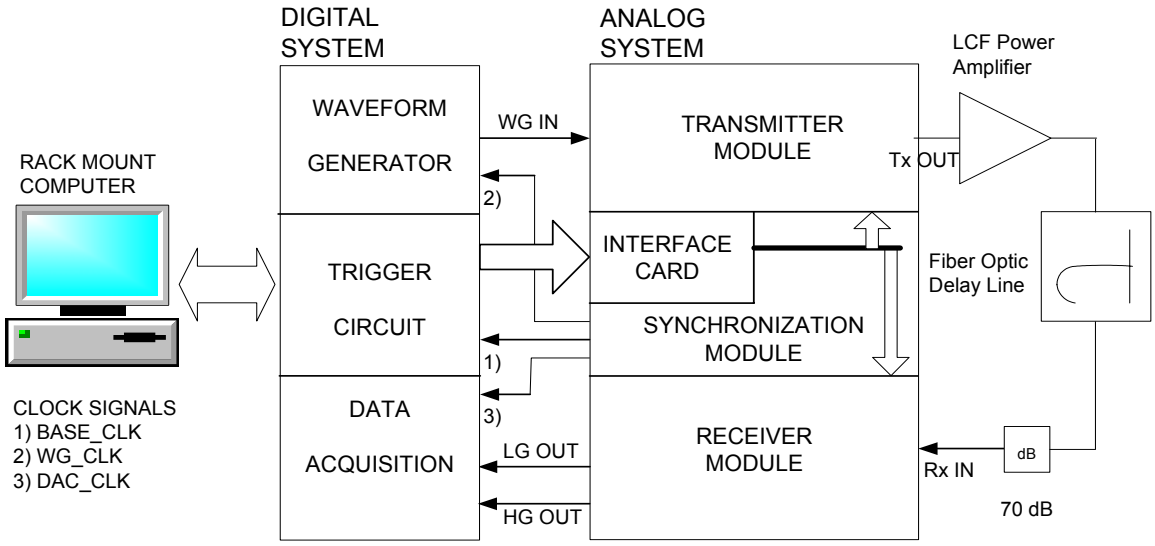

Figure 3.22: Experimental setup for a loop-back test of the ACORDS

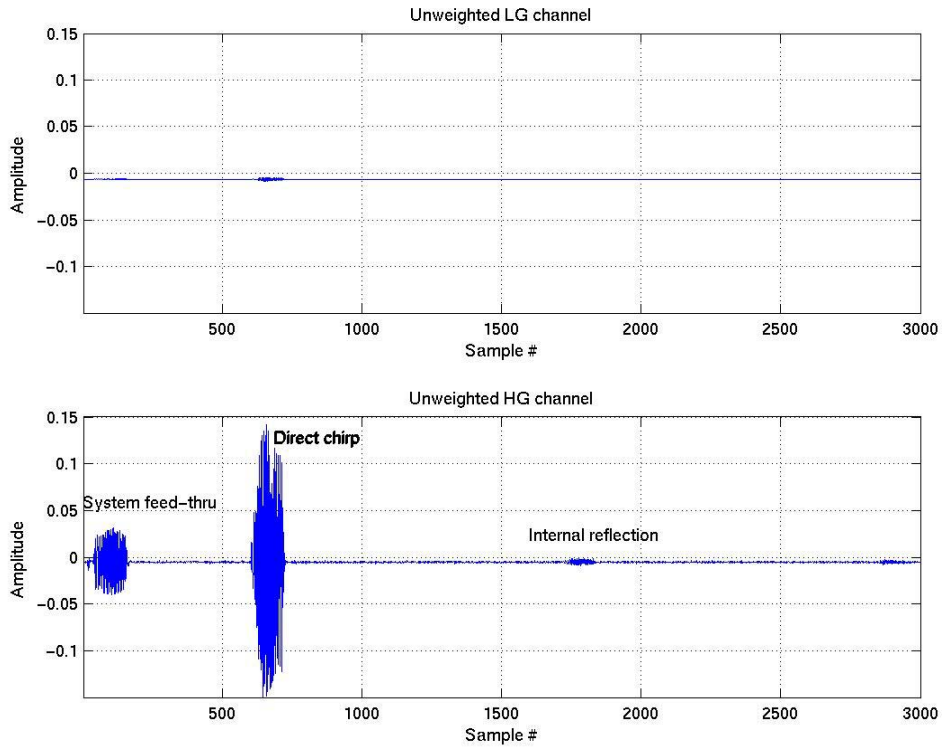

Figure 3.23: Digitized LG and HG channel

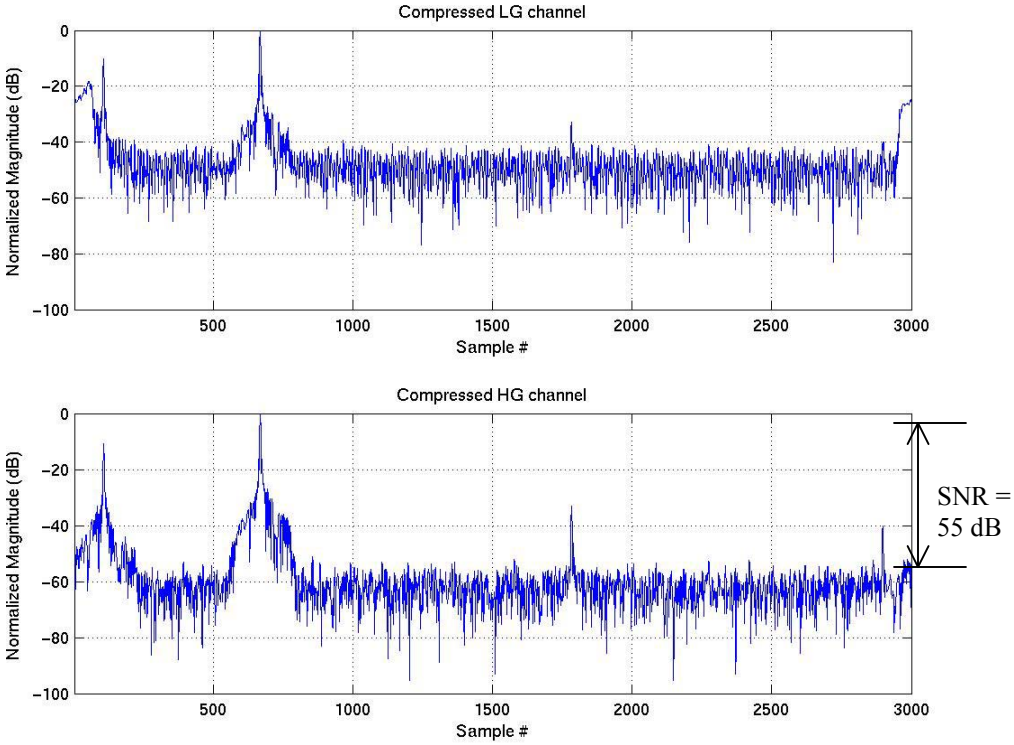

Figure 3.24: Compressed LG and HG channel

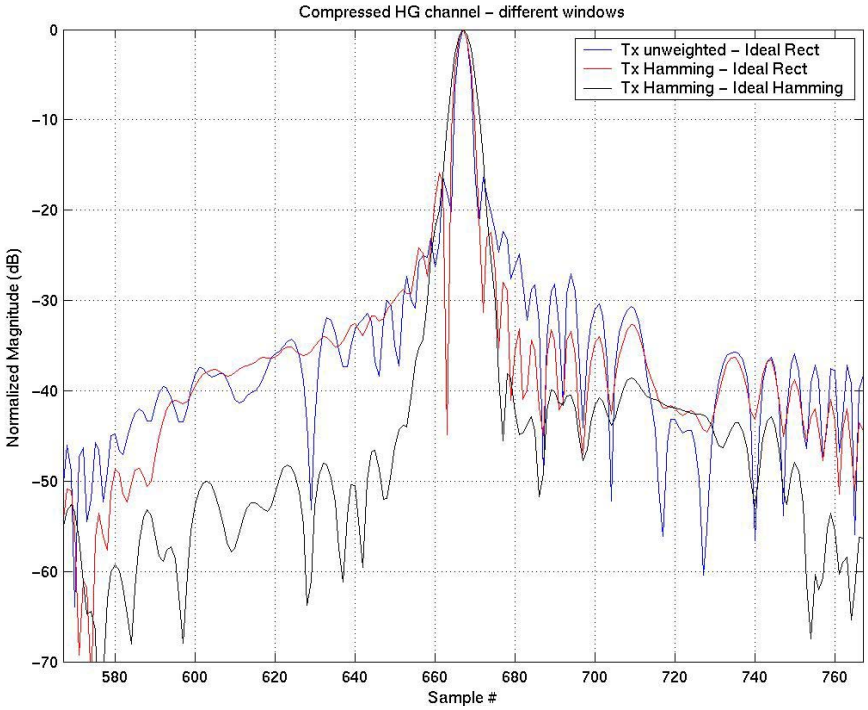

Figure 3.25: Compression results of HG channel for different windowing functions

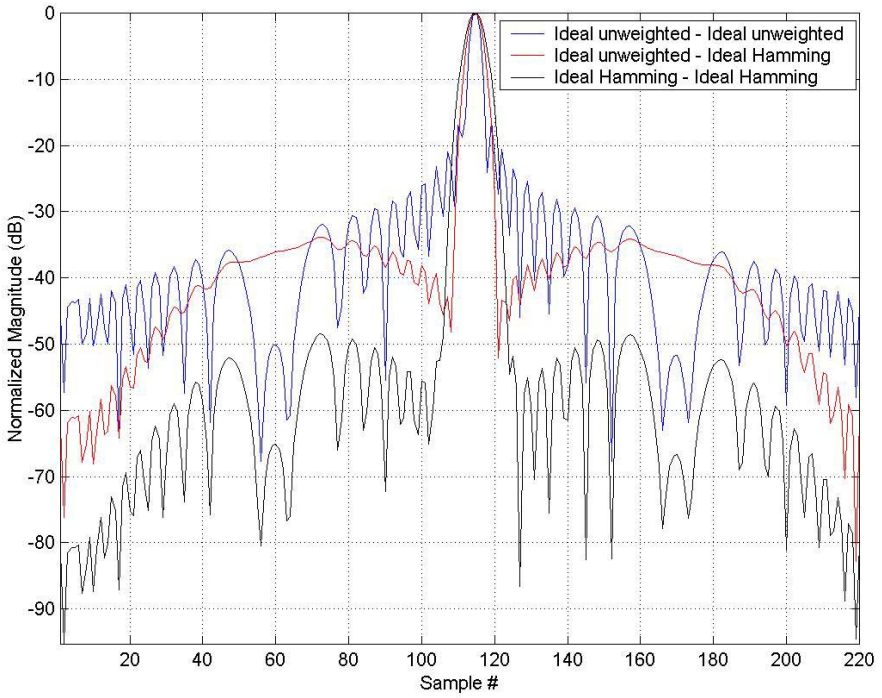

Figure 3.26: Compression results of ideal chirp for different windowing functions

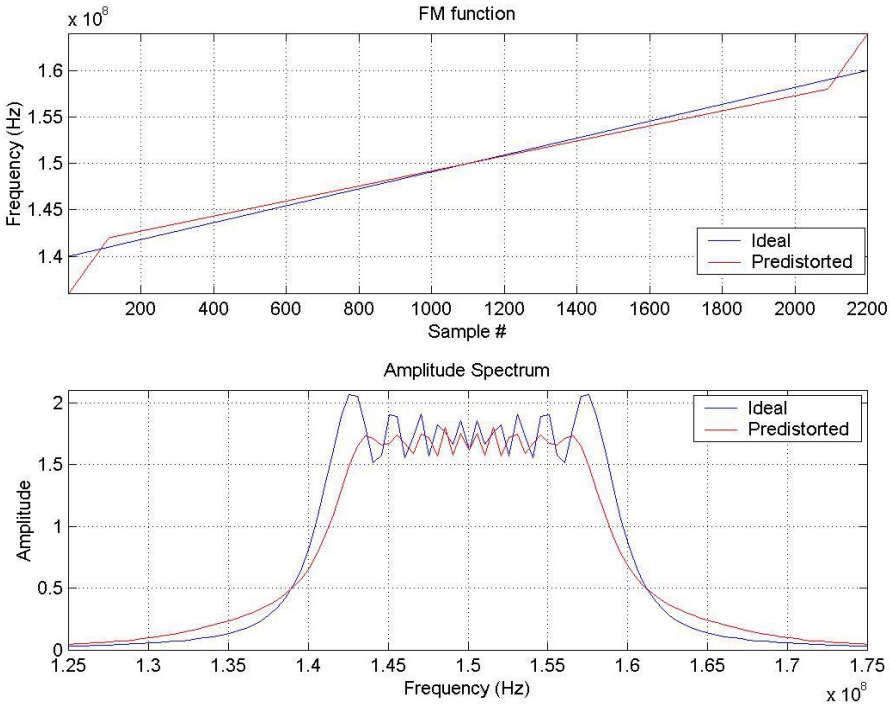

Figure 3.27: Comparison of simulated FM function (top) and amplitude spectrum (bottom)

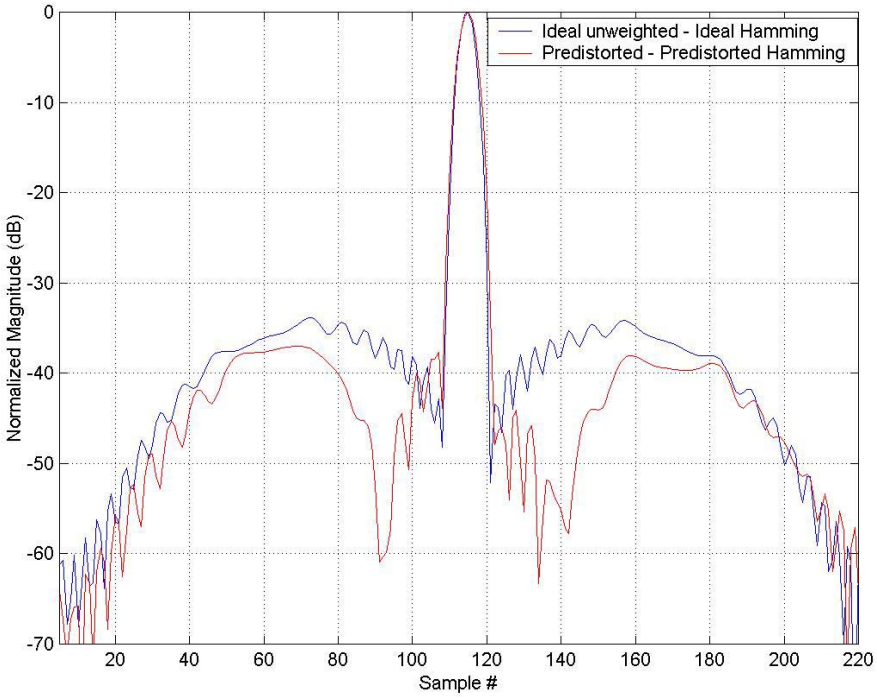

Figure 3.28: Compression result of ideal and predistorted chirp for Hamming window

CHAPTER 4

Field Experiment Results

4.1 Field test of radar system

The ACORDS system was tested in Greenland during the 2003 field season. The field experiment included six flightlines in the month of May. The system was installed on a NASA P3 aircraft at the NASA Wallops Space Flight Facility in Virginia. The system installation in the aircraft was similar to that of the NG-CORDS system. Figure 4.1 shows the ACORDS system after mounting inside the pressurized cabin of the NASA P3 aircraft.

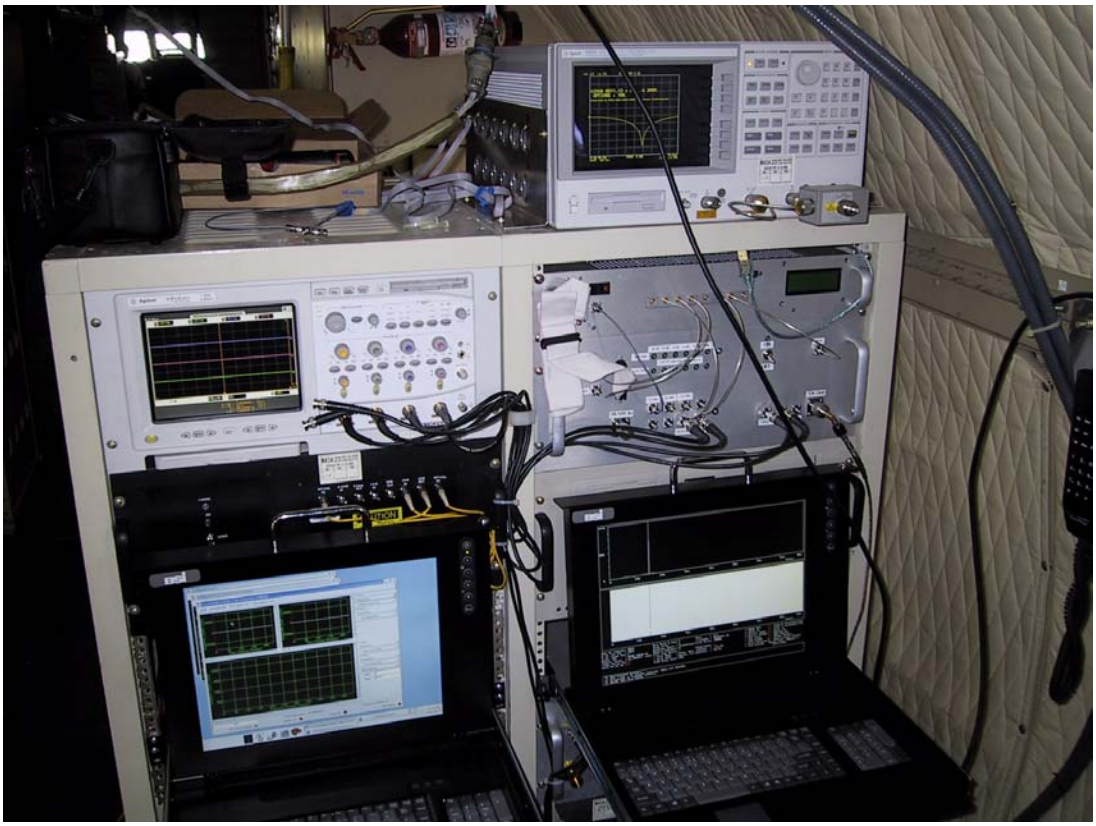

Figure 4.1: ACORDS system after mounting inside the pressurized cabin of the NASA P3 aircraft

4.2 Results

This section presents some results collected during the 2003 season using the ACORDS system. The common radar settings under which the radar was operated are shown in Table 4.1. These settings may differ depending upon the location, but they are all stored in the header of the raw data files. The attenuation in the LG channel was set such that the strong return from the air/ice interface did not saturate the LG channel. This way, the Rx Blank switch in the front end of the receiver was always operating in the ON mode. The attenuation in the HG channel was set such that there is a 30-dB overlap in the two gain channels.

Description	**Characteristic**	**Units**
Tx pulse width	3	µsec
Tx weighting	Hamming	-
Tx Blank 1	3	µsec
Tx Blank 2A	3	µsec
Tx Blank 2B	3	µsec
Rx Blank	0	µsec
High Gain Blank	5	µsec
Low Gain Atten	36	dB
High Gain Atten	20	dB

Table 4.1: Radar settings of ACORDS

Figure 4.2 shows the LG and HG radio echograms of a flightline in northern Greenland with good internal layering. The LG echogram has been compensated for the gain difference in the two channels. Due to less gain in the LG channel, the deep internal layers and weak returns are masked by the A/D noise, whereas in the HG

echogram, the HG Blank switch has attenuated the surface return and few internal layers. Thus the two channels need to be combined into a single channel that has a very high dynamic range. The integration can be done either coherently or incoherently. Coherently integrated radio echograms can be used for further processing as it still has the phase information, whereas incoherently integrated radio echograms are the last product. Figure 4.3 shows a coherently and incoherently integrated LG and HG echogram. Figure 4.4 shows the plot of the hundredth A-scope in the LG, HG and coherently integrated echogram. Figure 4.5 compares the same in the LG, HG and incoherently integrated echograms. The dynamic range in the A-scope of the integrated echograms is around 115 dB.

Figures 4.6 and 4.7 show the LG and HG radio echogram, respectively, of the Petermann Glacier. As there is no blanking involved in the LG channel, the LG echogram looks better than the HG echogram. The Calving Front is also shown in the two echograms.

The ACORDS was also operated over Jacobshavn Glacier in southern Greenland. In this region, the ACORDS was programmed to transmit a 10 μs radar pulse instead of a 3 μs pulse. This modification had improved the system loop sensitivity by 5 dB. Figure 4.8 shows a HG radio echogram of the Jacobshavn Glacier. The bedrock of the glacier cannot be seen as it is masked by clutter. Noise filtering techniques like wiener filtering and wavelet denoising were applied to reduce the clutter. Figure 4.9 shows a zoomed-in HG radio echogram of the glacier after filtering. The bedrock in the filtered echogram can be seen with the help of noise.

Figure 4.10 shows the ice thickness plot of the Jacobshavn glacier. The thickness of the glacier at the nadir is around 2.25 Km.

We were not able to sound the ice thickness of glaciers present further downstream. The main factors that hinder the performance of the system are the sloping nature of the bedrock and the higher loss due to temperate and wet ice. Figure 4.2 illustrates the problem caused due to the sloping nature of the bedrock.

The glacial bedrock is assumed to be a triangle. The sample points ‘a’ and ‘b’ are assumed to be two points present on the bedrock of adjacent amplitude scopes. The spacing between the two amplitude scopes depends on the velocity of the aircraft, pulse repetition frequency and the number of onboard pre-integrations. It can be seen that the two-way return paths for the sample points are different. The two-way phase shift between the two points has been calculated to be far greater than 45 degrees. It is known that the phase shift between adjacent samples for unfocussed synthetic aperture radar should be less than 45 degrees [24]. Therefore, any post-coherent integration would cause the sample points to add destructively, thereby cancelling out the bedrock in the channel. We cannot integrate them incoherently as the signal-to-noise ratio is less when compared to coherent integrations.

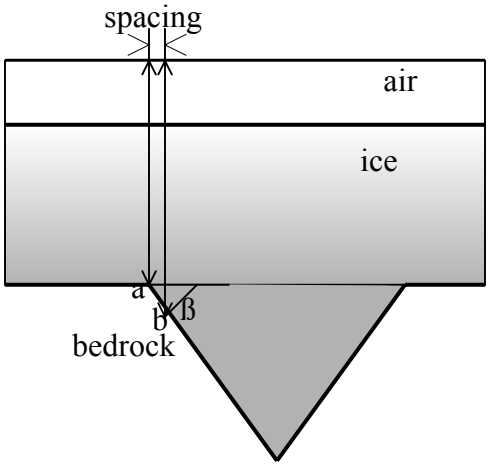

Figure 4.2: Illustration of the sloping nature of the bedrock

4.3 Summary of results

The ACORDS was tested successfully during the 2003 field experiment. It was shown that the LG and HG radio echograms could be integrated into an echogram that has a very high dynamic range. The data collected in this field experiment had good control over the gain, therby making the system deconvolution process easy.

The ACORDS was easy to control from an operator's point of view. The performance of the ACORDS over outlet glaciers was similar to that of NG-CORDS. In the case of outlet glaciers, we were able to sound the ice thickness of a glacier that was located upstream in the Jacobshavn region. We were not able to measure the ice thickness over downstream glaciers.

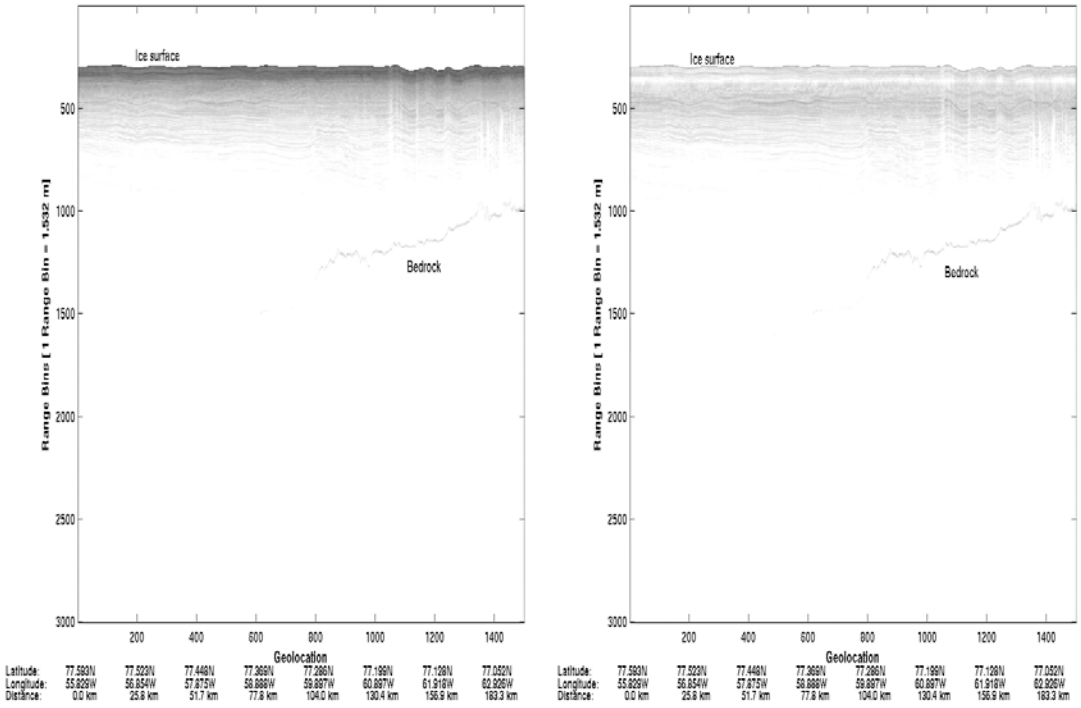

Figure 4.3: Radio echogram of LG (left) and HG channel (right) showing internal layers

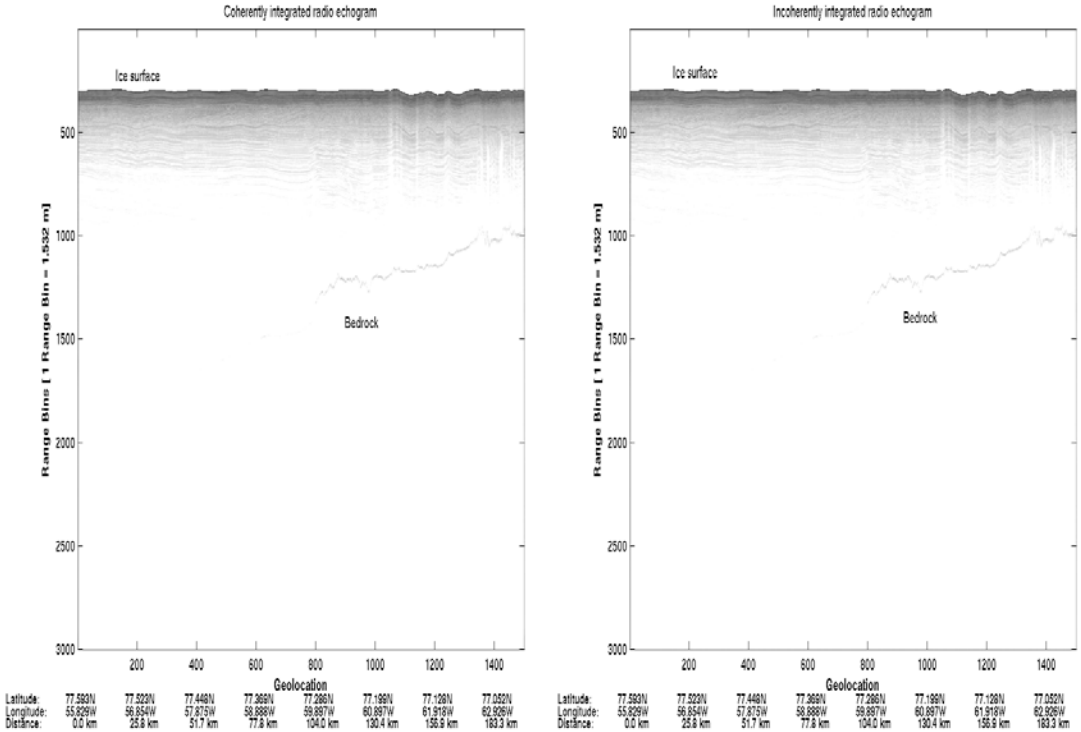

Figure 4.4: Radio echogram of coherently (left) and incoherently integrated (right) LG and HG channels

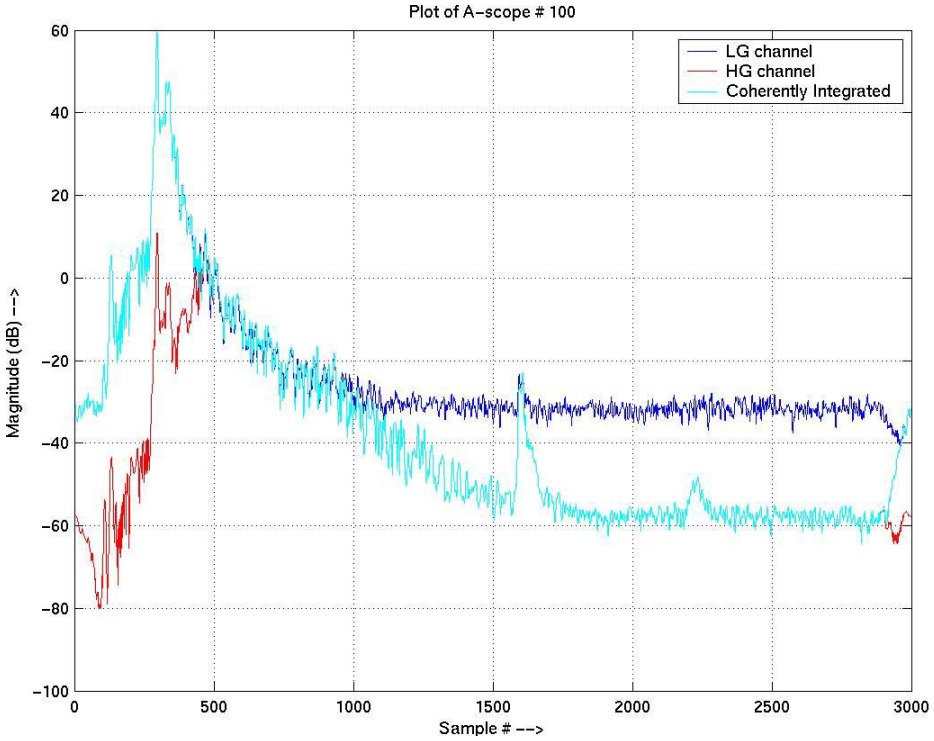

Figure 4.5: A-scope plot of LG, HG and coherently integrated echograms

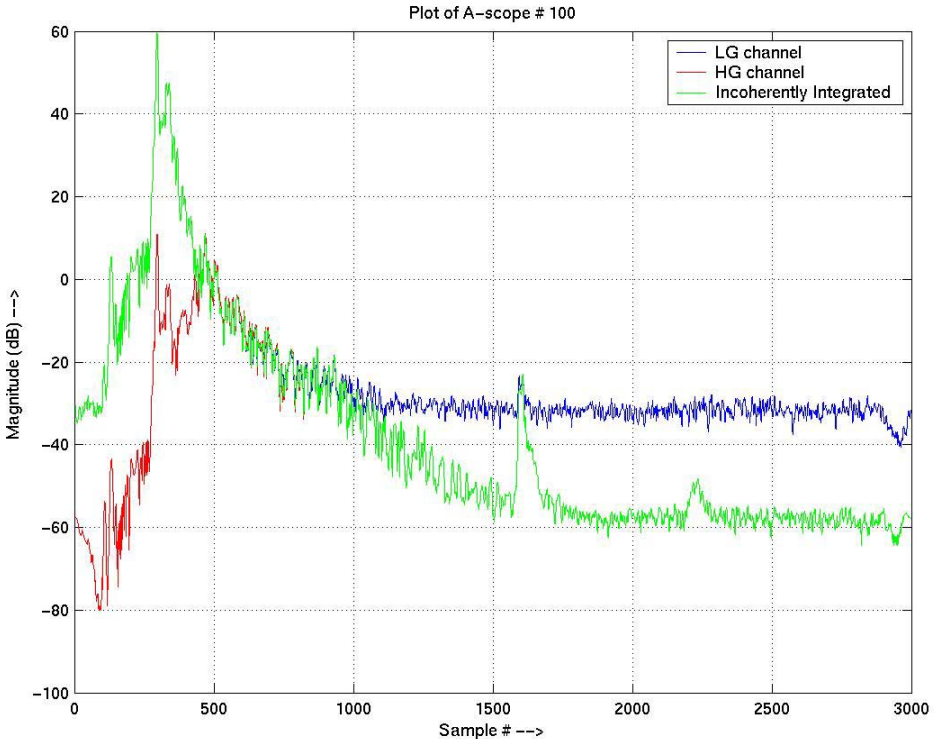

Figure 4.6: A-scope plot of LG, HG and incoherently integrated echograms

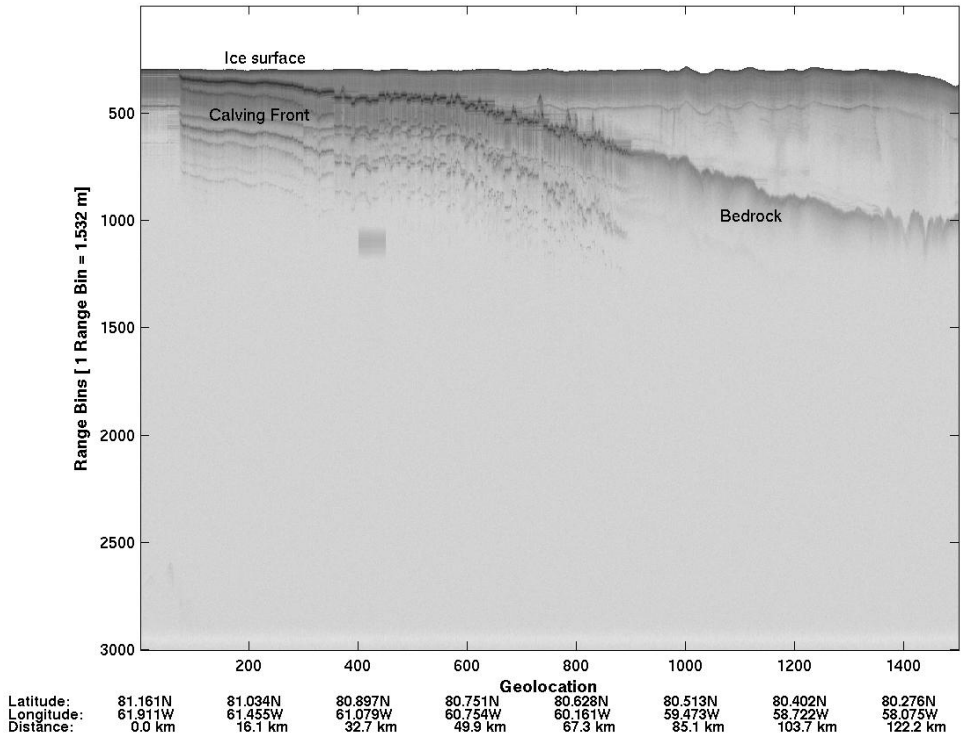

Figure 4.7: LG radio echogram of the Petermann Glacier

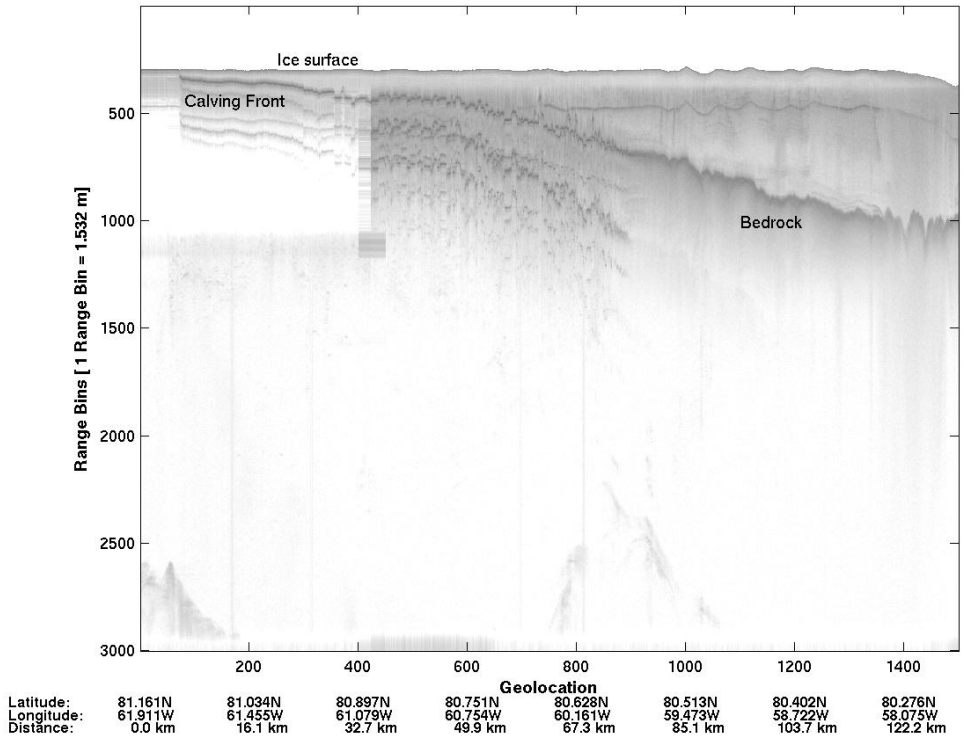

Figure 4.8: HG radio echogram of the Petermann Glacier

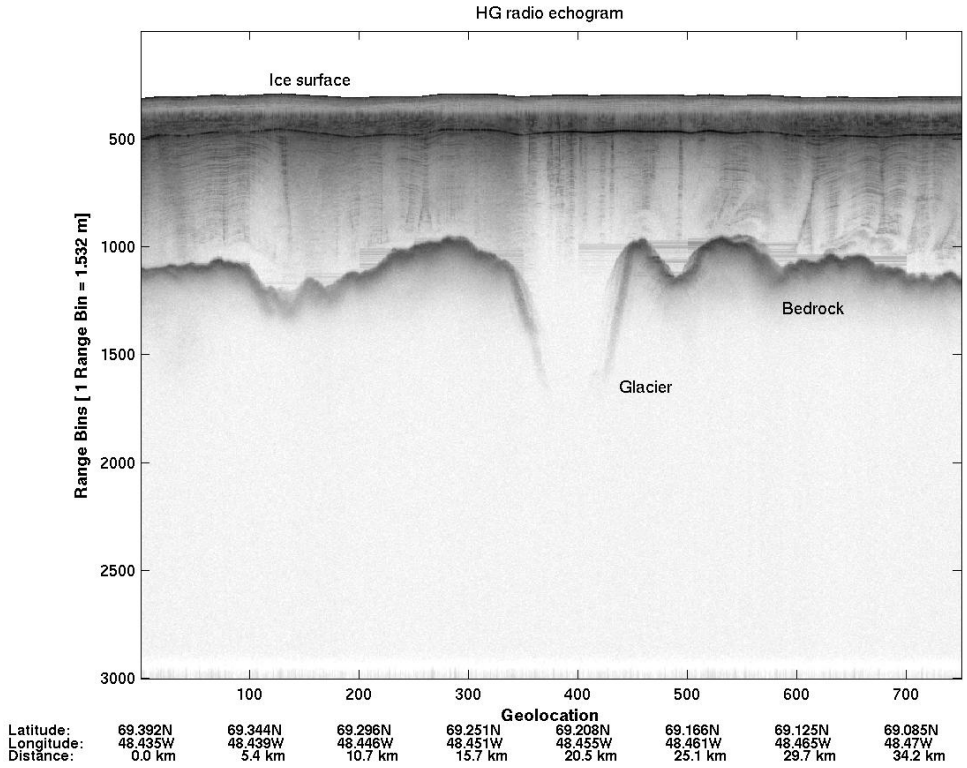

Figure 4.9: HG radio echogram of the Jacobshavn Glacier

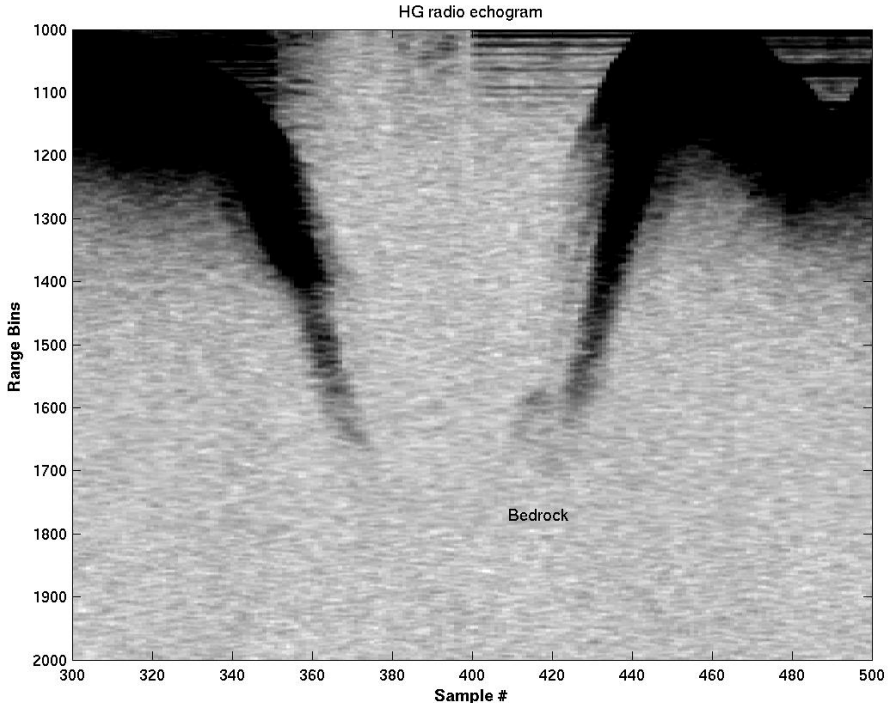

Figure 4.10: Zoomed in HG radio echogram of the Jacobshavn Glacier after filtering

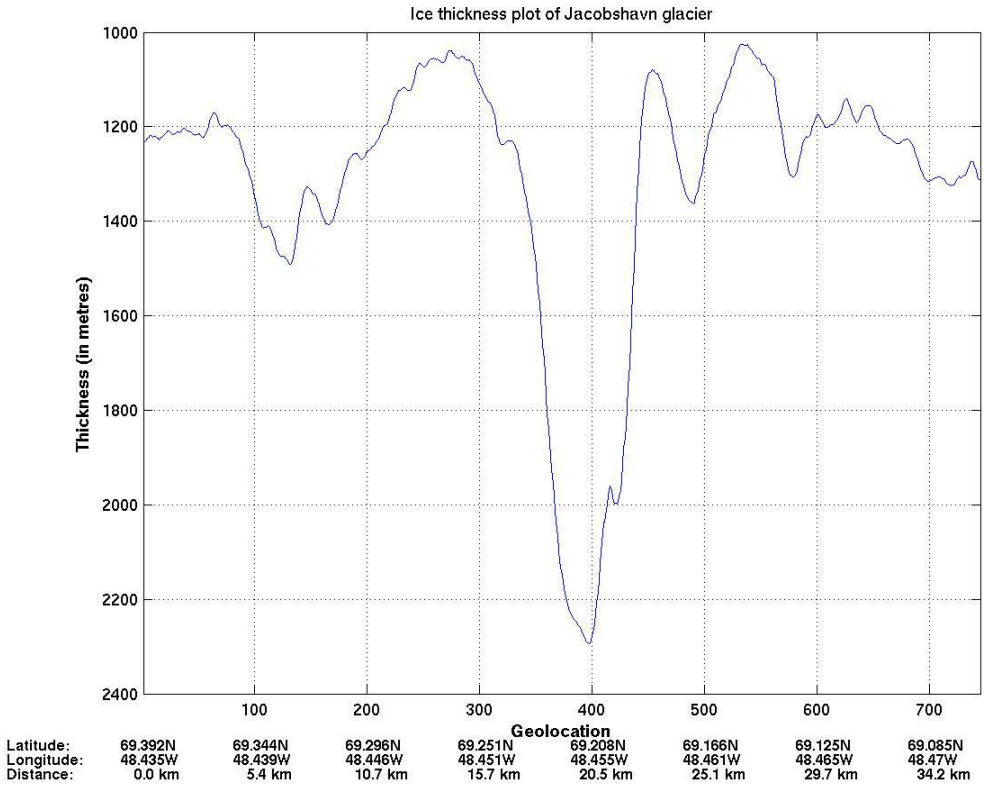

Figure 4.11: Ice thickness plot of Jacobshavn Glacier

CHAPTER 5

Conclusions and future recommendations

5.1 Conclusions

The ACORDS system was designed and developed to improve the performance of the NG-CORDS radar. The transmitter waveform for the ACORDS is generated digitally. The D/A converter in the waveform generator operates at a clock frequency of 110 MHz in an oversampling mode to generate the 140-160 MHz chirp waveform. The radar transmitter amplifies the chirp waveform to a peak power level of 200 W. It has been implemented on a two-layered printed circuit board of dimensions 3.6'' x 5.6''.

The dual-channel receiver consists of two different gain channels with individual gains of 44 dB and 80 dB respectively. The STC and the variable attenuator are replaced by a high-gain blanking switch and digital attenuator to achieve a high dynamic range. The dual-channel receiver is implemented on a two-layered printed circuit board of dimensions 3.6'' x 5.6''. A dual-channel A/D converter capable of undersampling at high frequencies is used to digitize the received RF signals, thereby getting rid of the I-Q demodulator. The A/D converter operates at a clock frequency of 55 MHz.

The advantages of the ACORDS over the NG-CORDS include the following:

- Range sidelobes of the received signals are reduced by weighting the transmit waveform.

- System loop sensitivity can be increased by increasing the transmit pulse width.
- There is good control over the gain in both the channels and hence easy to deconvolve the system response.

The ACORDS was successfully tested in Greenland during the 2003 field season. The ACORDS system was not successful in mapping the bedrock over the outlet glaciers in southern Greenland due to the sloping nature of the glacial bedrock. In these regions, where ice at the bedrock is temperate and wet (contains water), the two-way attenuation is higher than 80 dB. Thus, a system with more sensitivity needs to be designed.

5.2 Future recommendations

The performance of the ACORDS system can be further improved by using deconvolution techniques. Certain components, like the power amplifiers and the antennas, used in the ACORDS system are not exactly linear in the 140-160 MHz frequency range. Hence, there will be some amplitude and phase non-linearities that are incorporated into the received signal. These non-linearities degrade the sidelobe performance of the radar. Deconvolution techniques should be used to remove the effects of the non-linearities, but this will require the system transfer function. The transfer function of the whole radar system, including the antennas, can be measured by pointing them to a point target such as the ocean. Deconvolution techniques that use this system transfer function need to be implemented to correct for the system effects.

The 200-W power amplifier in the ACORDS is a separate module. It needs to be redesigned such that it can be integrated with the RF-section of the ACORDS transmitter. This will make the ACORDS system more compact.

For better performance of the ACORDS system over outlet glaciers, an algorithm that takes into account the slope of the bedrock before performing coherent integrations needs to be implemented. Reducing the number of onboard pre-coherent integrations to 32 or less and slope corrections will eliminate the problem due to the sloping nature of the bedrock. An extensive analysis needs to be done to simulate the two-way attenuation in ice using geophysical data such as temperature, water content, and acidity content. This will help to determine the additional loop sensitivity required to map the ice thickness in these regions.

Lowering the radar frequency and increasing the system bandwidth can also improve the performance of the ACORDS system over transition zones. Increasing the system bandwidth will improve the radar range resolution and also increase the pulse compression gain. Lowering the radar frequency will reduce the off-vertical surface clutter. Hence, a wideband depth sounder with lower radar frequency needs to be developed to improve the performance of the radar in regions masked by clutter.

REFERENCES

[1] Dyurgerov, M.B., and M.F. Meier, "Year-to-year fluctuations of global mass balance of small glaciers and their contribution to sea-level changes," *Arctic and Alpine Res*., 29(4), pp.392-402, 1997.

[2] Raju, G., W. Xin, and R. K. Moore, "Design, development, field observations, and preliminary results of the Coherent Antarctic Radar Depth Sounder (CARDS) of the University of Kansas, USA.," *Journal of Glaciology*, 36(123), pp.247-254, 1990.

[3] Xin, W., "Data processing system of the coherent antarctic radar depth sounder," *RSL Tech. Report 8070-3*, September 1989.

[4] Chuah, T.S., "Design and Development of a Coherent Radar Depth Sounder for Measurement of Greenland Ice Sheet Thickness," *RSL Tech. Report 10470-5*, January 1997.

[5] Akins, T., "Design and development of an improved data acquisition system for the coherent radar depth sounder," *M.S. Thesis*, Electrical Engineering and Computer Science, The University of Kansas, 1999.

[6] Gogineni, S., D. Tammana, D. Braaten, C. Leuschen, T. Akins, J. Legarsky, P. Kanagaratnam, J. Stiles, C. Allen and K. Jezek, "Coherent radar ice thickness measurements over the Greenland ice sheet," *Journal of Geophysical Research* (*Climate & Physics of the Atmosphere*) special issue on PARCA, 2001.

[7] Joughin, I., M. Fahnestock, R. Kwok, P. Gogineni and C. Allen, "Ice flow of Humboldt, Petermann and Ryder Gletscher, northern Greenland," *Journal of Glaciology*, vol. 45, no. 150, pp.231-241, 1999.

[8] Stimson, George W., *Introduction to Airborne Radar*, second ed., Scitech Publishing, Inc., Mendham, New Jersey, 1998.

[9] *Pulse Expansion and Compression Subsystem*, PHONON Corporation, Simsbury, CT, 1995.

[10] Skolnik, M.I., *Introduction to Radar Systems*, third ed., McGraw Hill, New York, 2001.

[11] Harris, F.J., "On use of Windows for Harmonic Analysis with the Discrete Fourier Transform," *Proceedings of the IEEE*, vol. 46, no. 1, January 1978.

[12] Tammana, D., "Design of Waveform Generator for Coherent Radar Depth Sounder," *M.S. Thesis*, Electrical Engineering and Computer Science, The University of Kansas, 2001.

[13] Robertson, D., "Selecting Mixed-Signal Components for Digital Communications Systems-Part V," Analog Dialogue, vol. 31, no. 3, 1997.

[14] Proakis, J.G., D.G. Manolakis, *Digital Signal Processing*, Prentice Hall, Englewood Cliffs, New Jersey, 1997.

[15] Lyons, R.G., *Understanding Digital Signal Processing*, Addison-Wesley Publishing Company, Reading, Massachusetts, 1997.

[16] Wehner, D.R., *High-resolution radar*, second ed., Artech House, Inc., Norwood, Massachusetts, 1995.

[17] Protel International Pvt. Ltd., *Protel 99 Designer's Handbook*, Protel Technology Inc., CA, USA, 1998.

[18] *Resin Sealed Bolt-in Filters*, Spectrum Control, Inc., Fairview, PA.

[19] Ott, H.W., *Noise Reduction Techniques in Electronic Systems*, second ed., Wiley, New York, 1976.

[20] *Minibend Coaxial Cable*, Astrolab, Inc., Warren. New Jersey.

[21] *5000 Series Fiberoptic Delay Line*, Ortel Corporation, Alhambra, CA, 1990.

[22] Misaridis, T.X., J.A. Jensen, "An effective coded excitation scheme based on a predistorted FM signal and an optimized digital filter," *IEEE Ultrasonics Symposium*, vol. 2, pp. 1589-1593, 1999.

[23] Cook, C.E., J. Paolillo, "A pulse compression predistortion function for efficient sidelobe reduction in a high-power radar," *Proceedings of the IEEE*, vol. 52, no. 4, April 1964.

[24] Ulaby, F.T., R.K. Moore, A.K. Fung, *Microwave Remote Sensing- Active and Passive,* vol. II, Artech House, Inc., Norwood, Massachusetts, 1982.